Development of Miniaturized Microbial Fuel Cell for Electricity Generation from Waste

to be submitted in partial fulfilment of the requirement for the degree of

Master of Technology

In

Biomedical Engineering

Submitted by

Rahul Kandpal
(2K15/BME/05)
Delhi Technological University, Delhi, India

under the supervision of

Prof. Bansi .D. Malhotra
Department of Bio-Technology
Delhi Technological University Delhi-110042
(Formerly Delhi College of Engineering, University of Delhi)

DECLARATION

I certified that the project report entitled **"Development of Miniaturized Microbial Fuel Cell for Electricity Generation from Waste"** submitted by me is in partial fulfilment of the requirement for the award of the degree of Master of Technology in Biomedical Engineering, Delhi Technological University. It is a record of original research work carried out by me under the supervision of **Prof. Bansi D. Malhotra,** Department of Biotechnology, Delhi Technological University, Delhi.

The matter embodied in this project report is original and has not been submitted for the award of any Degree/Diploma.

Date:

Rahul Kandpal
2k15/BME/05
Department of Biotechnology
Delhi TechnologicalUniversity
Delhi-110042

CERTIFICATE

This is to certify that the project entitled **'Development of Miniaturized Microbial Fuel for Electricity Generation from Waste'** submitted by Rahul Kandpal (Roll No. 2K15/BME/05) in the fulfillment of the requirements for the reward of the degree of Master of Technology in Biomedical Engineering, Delhi Technological University, Delhi-110042 is an authentic record of the candidate's own work carried out by him under my guidance. The information and data enclosed in this thesis is original and has not been submitted elsewhere for honoring of any other degree.

Date:

Prof. D. Kumar
(Co- Project Mentor & Head)
Department of Biotechnology
Delhi Technological University
Delhi-110042

Prof. Bansi D. Malhotra
(Project Mentor)
Department of Biotechnology
Delhi Technological University
Delhi- 110042

ACKNOWLEDGEMENT

I hereby express my profound sense of reverence of gratitude to my supervisor and mentor, ***Prof. B.D. Malhotra, Department of Biotechnology, Delhi Technological University, Delhi-110042*** who has guided me through thick and thin. Without his valuable guidance, incessant help, calm endurance, constructive criticism, and constant encouragement the completion of this minor project would have been impossible, the congenial discussion with him made me confident and gave enough independence in performing the experiment which enabled in me a higher efficiency to complete the work.

I express my kind regard and gratitude to ***Prof. D. Kumar*** (HOD, Department of Biotechnology), and all faculty members for helping in my project.

I highly indebted to ***Dr. Sharda Nara*** (Post Doctoral Research Scholar), ***Dr. Suveen Kumar and Dr. Saurabh Kumar*** (Research Scholar) for their guidance and constant supervision as well as for providing necessary information regarding the instruments and experiments and also for their support in completing the reports. I am highly grateful to ***Ms Shine Augustine*** (Research Scholar) for her valuable suggestion and guidance during the entire tenure of my dissertation work.

I would like to thank my colleagues ***Anas Saifi***, ***Ratan Kumar*** and ***Tarun Narayan*** for their great help and support to conduct my research.

I would also like to thank ***Mr. Chhail Bihari***, ***Mr. Jitender Singh*** and ***Mr. Mukesh Kumar*** for providing necessary and maintaining laboratory in good condition.

At last but never the least, words are small trophies to express my deep sense of gratitude and affection to my loving friend and my parents who gave me infinite love to go for this achievement.

Rahul Kandpal

2K15/BME/05

M.Tech. (Biomedical Engineering)

CONTENTS

List of Abbreviations

µA	Micro-Ampere
CE	Counter Electrode
MFC	Microbial Fuel Cell
CV	Cyclic Voltammetry
EDC	N'-ethyl-N-(3-dimethylaminopropyl) carbodimide
NHS	N-Hydroxysuccinimide
EIS	Electrochemical Impedance Spectroscopy
$[Fe(CN)_6]^{4-}$	Ferrocyanide
$[Fe(CN)_6]^{3-}$	Ferricyanide
rGO	Reduced Graphene Oxide
GO	Graphene Oxide
PBS	Phosphate Buffered Saline
SEM	Scanning Electron Microscopy
TEM	Transmission Electron Microscopy
V	Volt
R_{CT}	Charge Transfer Resistance (Nyquist diameter)

List of Tables

List of Schemes/Figures

CHAPTER-1

Development of Miniaturized Microbial Fuel Cell for Electricity Generation from Waste

Rahul Kandpal

Delhi Technological University, Delhi, India

Email Id: kandpal22rahul@gmail.com

1. Abstract

Microbial fuel cells (MFCs) are known to convert chemical energy stored in organic matter to electrical energy by microbial electrochemical reactions. The present studies deal with the fabrication of two types of MFCs viz. H-shaped and miniaturized MFCs using low cost materials. H-shaped MFC shown open circuit voltage (OCV) of 750 mV after 42 days while miniaturized MFC depicted OCV of 671.2 mV only after 15 hrs. Aluminium sheet (Al) coated with graphite paste (G), polyaniline (PANI), reduced graphene oxide (rGO) were used as electrode materials while agar gel was employed as proton exchange material. Comparison of different electrode materials (G/Al, rGo/G/Al, PANI/rGO/G/Al) was evaluated using cyclic voltammetry, four points probe conductivity and scanning electron microscopy (SEM). rGo/Graphite paste/Al was found the most appropriate electrode material with conductivity of 0.52 S/m, addition of rGO enhanced the conductivity upto 19.40 % to that of G /Al. Fermenting bacteria present in kitchen waste (potato slurry) were used in anode chamber as a main source for electricity generation. Furthermore, effect of adding real saliva, artificial saliva to anolyte and salivary enzymes (lysozyme and α-amylase) immobilization on anode surface were also observed. Instantaneous enhancement of potential was attained after adding saliva. Similar results were obtained when study was conducted with the electrodes having immobilized salivary enzymes while no substantial increase in current was observed when only artificial saliva was used. Thus, miniaturized MFC developed using

rGO/G/Al as electrode material and natural saliva as supplement to anolyte gave OCV of **671.2 mV**, maximum current of **53 µA** across 10 kΩ load and internal resistance of **1042.35 Ω** with a shelf life of **40 days**. Thus, assembly of 3 to 4 such miniaturized MFCs could able to generate electricity required for biosensors and light emitting devices (LEDs).

Keywords: MFC, PANI, rGO, Anolyte.

CHAPTER-2

2. Introduction

Electricity is regarded as one of the basic needs an individual requires on a daily basis. Our basic power requirements are fulfilled by coal-based power plants, which are a matter of environmental concern. Coal and other non-renewable power sources will deplete someday. Therefore, there is a need to shift from non-environment friendly to environment-friendly sources of energy. We have done much progress in this field and we have many new alternatives of energy generation like wind turbines, hydro power plants in dams, hydrogen fuel cells, solar energy from solar cells and nuclear energy. There is another emerging technology known as microbial fuel cells (MFC) which convert chemical energy from biodegradable organic matter into electricity by using microbial metabolism. It means that we can convert organic waste from household into electricity. A microbial fuel cell comprises of two chambers i.e. an anode chamber and a cathode chamber. An anode chamber contains a highly conductive anode of high surface area and an anolyte (wastewater) whereas cathode chamber contains a conductive cathode and catholyte (containing electron acceptors).

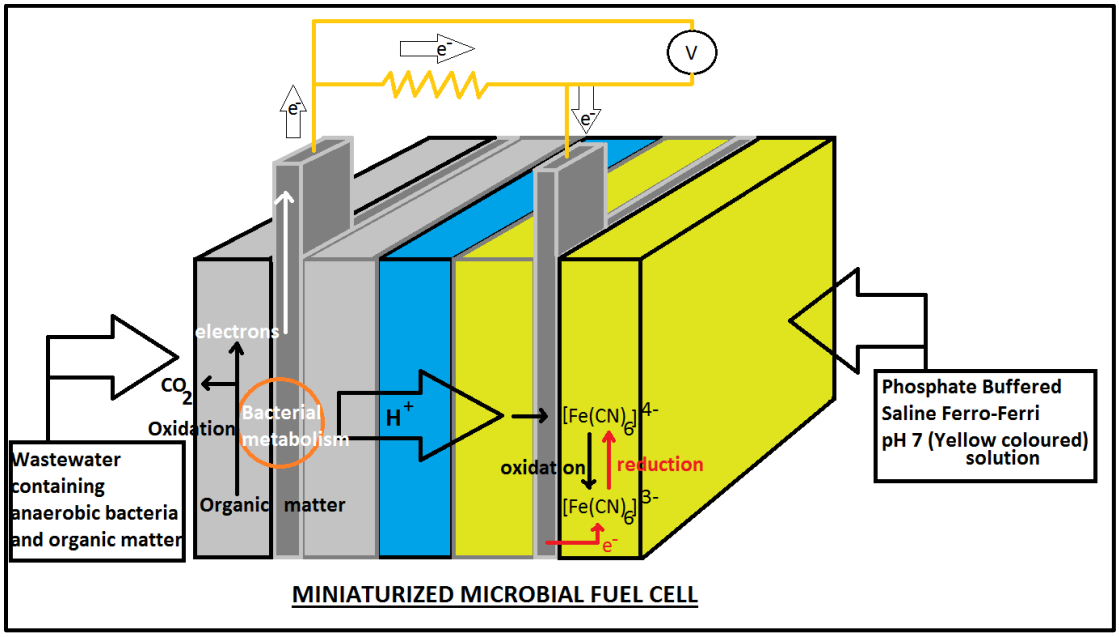

Figure 2.1 Miniaturized Microbial Fuel Cell

Both these anode and cathode chambers are separated by a proton exchange membrane which transports protons (H^+) from anode chamber to cathode chamber. Anaerobic bacteria from wastewater attach on the surface of conductive anode and oxidize the organic matter present on wastewater to release electrons on the anode surface. These electrons transfer from anode to cathode via an external conductive load and the protons released from the microbes transfer to the cathode chamber via proton exchange membrane and at last an electron acceptor present in the catholyte gets reduced by accepting electrons coming from the anode. This process completes the circuit and as a result electricity is produced. But the problem lies in the amount of electricity produced which is too small (~3-4 W/m^2) so miniaturized MFCs could be used to generate enough power for small sensors or diagnostic devices. The power generated from small MFCs ranges from 0.4 $\mu W/cm^2$ to 1 mW/cm^2 which is high enough to be used in small sensors or diagnostic devices. But the main problem in fabrication of these MFCs is their cost which is very high and the reason for this high cost being expensive fabrication techniques, materials of anode and cathode and the use of expensive proton exchange membranes (eg: Nafion 116 membrane from Dupont). Hence in order to utilize this technology fully its cost is needed to be reduced. This could be done by the use of low-cost materials for anode, cathode and proton exchange membrane.

We have developed a miniaturized MFC with very low production cost. The PEM used was made of agar gel. The anode/cathode electrodes were made up of aluminum coated with graphite paste, reduced graphene oxide(rGO)/graphite paste/Al and Polyaniline (PANI)/rGO/Graphite paste/Al. Both these electrodes and PEM were surrounded by hydrophobic barrier made up of wax. This low-cost miniaturized MFC could be used as a power source for diagnostic devices in developing countries.

CHAPTER-3

3. Literature Review

The literature review provides the related information regarding the MFC technology and will give the bibliophile a broad understanding of its function, design and potential marketable use in the real world. This sketches several features of the technology and will explore its practicality in industrial applications based on the newest research and experiments conducted by other scientists in this area.

3.1 Microbial Community

Understanding the basic functions of bacterial community is necessary in order to understand MFCs. Bacteria oxidize the organic matter present in the media in which it is grown, in order to derive as well as release energy from it. An additional attention will be given to a special type of bacteria that releases some electrons towards an anode of an MFC. Such bacteria are termed as exoelectrogens, “exo” meaning exocellular and “electrogens” meaning having an ability to transfer electrons to the anode or any other conducting surface over which they are grown. Many anaerobic bacteria can transfer electrons only to soluble compounds (nitrate and sulfate) which are not cell synthesized, diffusing across the cell membrane into the cell. Exoelectrogenic bacteria due to their ability to release electrons are the most suitable class of microbes which can work with MFCs to provide the maximum power output. Bacteria of such type are used in ‘mediator-less MFCs’, which do not require mediators to help with the electron transfer. Some examples of mediators are methylene blue, pyocyanin, thionin etc.[1] According to Du et al, these exoelectrogens are found in marine sediment, soil, wastewater, activated sludge and freshwater sediment, rich in these microorganisms.[1] In recent studies it was found that fungi can act as a mediator and as a result

it increases stability in electron transfer. This relationship found between exoelectrogens and fungi could potentially be helpful to scale up MFCs due to their presence naturally.[2]

3.2 Principle of Microbial Fuel Cell (MFC)

"Microbial fuel cells (MFCs) are bioelectrochemical systems that use the metabolism of microbes to oxidise fuels, generating current by mediated or direct electron transfer to the MFC electrodes."[3], [4] The device comprises of following components:

1. Cathode chamber: Containing Cathode and catholyte
2. Anode Chamber: Containing Anode and Anolyte
3. Proton exchange membrane (PEM)
4. External Circuit

MFC converts biodegradable organic matter directly into electricity. [5] Anode contains biodegradable organic matter and bacteria (anolyte) in an anaerobic environment. The cathode contains catholyte which may be conductive saltwater containing oxygen as an electron acceptor or phosphate buffered saline ferrocyanide-ferricyanide solution where ferricyanide acts as an electron acceptor in a double chamber type MFC or air the MFC is single chamber MFC. The bacteria releases protons and electrons as the biodegradable organic matter is converted into energy. The energy generated by microbes is used for growth and multiplication. The electrons generated are transferred directly to the MFC anode (in a mediator-less MFC setup) and to the cathode electrode the external circuit containing a conductive material. Protons pass through the proton exchange membrane from the anode chamber to the cathode chamber to produce water if oxygen is the electron acceptor or ferricyanide from ferrocyanide if ferricyanide is the electron acceptor as a result of the reduction process occurring due to the result of proton transfer. [6]

Reaction occurring at cathode in different MFCs

1. With O_2 as electron acceptor

$$4H^+ + 4e^- + O_2 \rightarrow H_2O$$

2. With ferricyanide as electron acceptor

$$\{Fe[CN_6]\}^{3-} + e^- \rightarrow \{Fe[CN]_6\}^{4-} + H^+$$

Direct electron transfer is not exhibited by all of the bacterial species except exoelectrogens, therefore using chemicals such as "methyl viologen, thionine, methyl blue, neutral red, and humic acid" is required. These chemicals are called redox mediators.

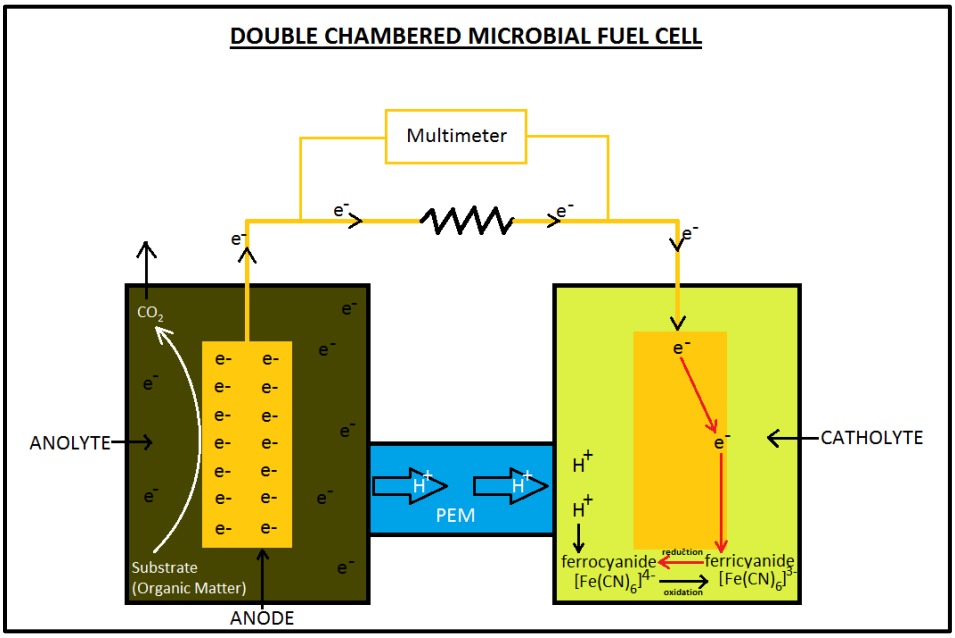

Figure 3.1 Schematic of the basic components of a MFC [7]

According to Logan et. al., the bacterial growth occurs in the anode, oxidising the organic matter by its breakdown into simpler products and releasing electrons. In order to effectively

transfer the electrons to the anode some bacteria are exoelectrogenic and hence forms biofilms over the anode surface to transfer electrons whereas others use mediators to transfer the electrons. The cathode is supplied with air containing oxygen or other electron acceptor like ferricyanide in order to complete the circuit and produce the required power.[7]

Chemical energy present in the organic matter is converted into electricity with the help of microbes releasing hydrogen ions and. The oxygen or ferricyanide is supplied in the cathode chamber. Electrode materials significantly influences the overall efficiency of the MFC.

3.3 Components

The microbial fuel cell consists of the following components in order to excellently harness energy, they are:

1. Anode and Cathode electrodes made of different conducting materials
2. Substrate: Substrate is any organic matter which could be used as an energy source.
3. Proton Exchange Membrane: different membrane materials like Nafion 117 from Dupont, agar gel membrane and PEDOT PSS membranes are used as PEM out of which Nafion is the most resistive of them all.
4. Bacteria: out of which exoelectrogens are mostly used in MFCs.

In order to optimize the overall efficiency of bioelectrochemical system (MFC), its each and every component needs to be improved.

Table 3.1 Basic components of MFC

Sr. no.	Item	Material	Remarks
1	Anode	Carbon-paper, carbon-cloth, Graphite-felt, Graphite, Platinum, Platinum-black, Reticulated vitreous carbon (RVC)	Necessary
2	Anode Chamber	Plexi-glass, polycarbonate, glass	Necessary
3	Cathode	Carbon-paper, carbon-cloth, Graphite-felt, Graphite, Platinum, Platinum-black, Reticulated vitreous carbon (RVC)	Necessary
4	Cathode Chamber	Plexi-glass, polycarbonate, glass	Optimal
5	Proton Exchange Membrane	Porcelain septum, nafion, agar-gel membrane	Necessary
6	Electrode Catalyst	Fe^{3+}, MnO_2, Pt black, Pt, Polyaniline, electron mediator immobilized on anode	Optimal

3.3.1 Electrodes

A number of factors determine the efficiency of an MFC and one of them is the material of the electrode. In order to improve the performance of MFCs many designs of MFCs have been tested. Balance of material cost and performance is a matter of challenge in the field of MFC technology. This report explores the advantages and drawbacks of different electrode materials that are widely used today, in terms of:

- conductivity

- surface properties
- biocompatibility
- cost[8]

The most effective electrodes are those which have the least resistance. “The resistance of the anode contribute majorly to the overall cell resistance of the MFC”[9]. However, using materials like platinum may improve the overall efficiency of MFC but it hampers the MFC cost which is a big issue if we want to scale-up our MFC. Characteristics like mechanical strength and high conductivity are important for an effective electron transfer. Since bacteria can also transfer electrons via different mechanisms other than direct electron transfer. Therefore, requirement for bacterial adhesion is not a must. Factors like scalability and cost-effectiveness also important. [8]

Some of the MFC studies are shown in Table 3.2.

Table 3.2 MFC studies on different electrode materials[33]

Sr. No.	**Electrode Materials**	**Configuration**	**Electrode Size**	**Inoculation Source**	**Reactor Configuration**	**Maximum Power/Current density**
1	Carbon (cloth)	Plane	7 cm^2	Preacclimated bacteria from an active MFC	Single chamber cube air-cathode MFCs	46 W/m^3 (volume) [34]
2	Carbon (paper)	Plane	22.5 cm^2	Primary clarifier overflow	Two-chamber, air cathode	600 mW/m^2 [5]
3	Carbon (mesh)	Plane	155 cm^2	Shewanella oneidensis	Two-chamber, air cathode	893 mW/m^2 (anode area) [35]
4	Carbon (granular)	Packed	450 ml	Domestic Wastewater	Single-chamber	5 W/m^3 (volume)

					cylindrical MFC	
5	Metal (plate)	Plane	0.12 m^2	Marine sediments	Artificial marine MFC	23 mW/m^2 (area)
6	Carbon (brush)	Brush	4 cm long by 3 cm in diameter	Preacclimated bacteria from an active MFC	Single chamber cube air-cathode MFCs	2400 mW/m^2 (anode surface area)

Commonly used MFC electrode materials are mostly carbonaceous due to their "good chemical stability, good biocompatibility, high conductivity, low cost and high surface area."[36]

MFC experiments use materials which include materials like carbon and metals like platinum, aluminium etc. It is well known that concentrationand type of bacteria on anode greatly affects the current density and power density in MFCs. Some of these materials are shown in figure 3.2. Mixed cultures in most of the MFCs are obtained from activated sludge or domestic wastewater. Increasing the surface area of anode is a major concern in MFCs and hence different configurations are used in order to do so. They are:

- Plane structure
- Packed structure
- Brush structure

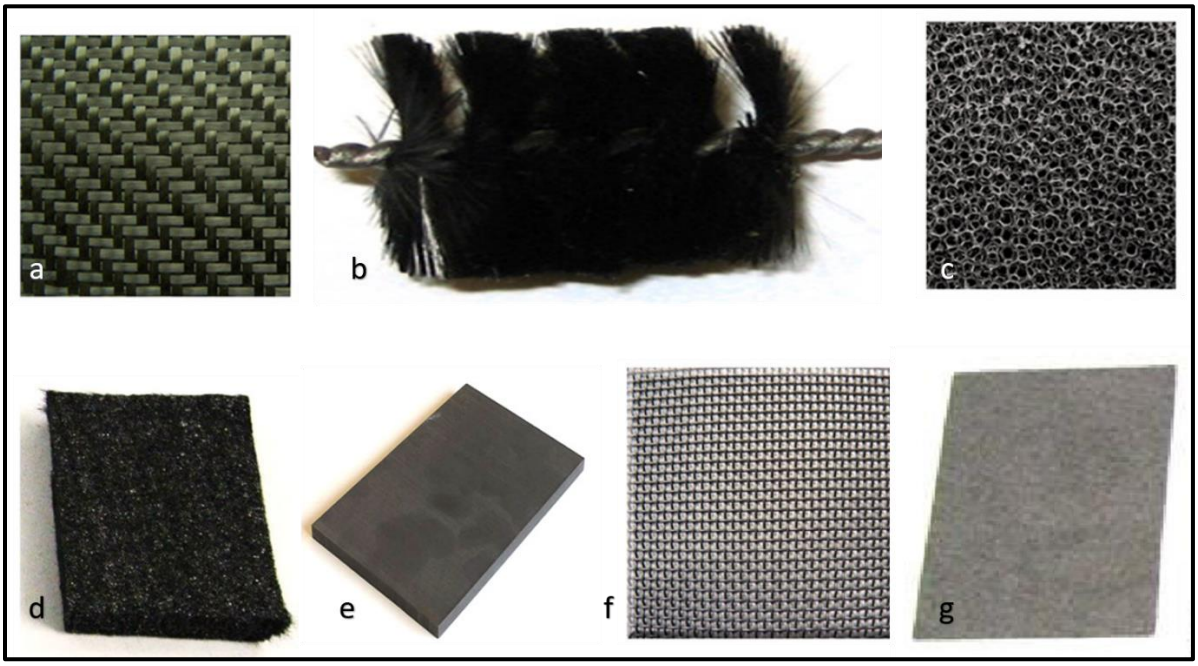

Figure 3.2 (a) Carbon mesh (b) Carbon brush (c) Reticulated vitrified carbon (d) Carbon felt (e) Graphite plate (f) Stainless steel (g) Carbon paper [16]

Plane structure:

Materials used in plane electrodes include: graphite plates, carbon paper, carbon mesh etc. Carbon paper is a brittle material and is very stiff and thin. Wei et al, used roughened graphite plate electrodes yielding a higher power density due to increased surface area of the rough electrodes than smooth graphite plates. Large scale application of these materials is not feasible due to its high cost and overall low specific area. Carbon mesh is used as an alternative due to low cost.[10] Fibrous materials like graphite foil and carbon cloth yield higher power generation due to their high absorption capacity and specific surface.

Packed structure:

In order to increase the surface area of the anode to attach bacteria, carbon materials in packings is used[19]. Anode chamber is filled with granular packing with its high specific area as

its main advantage. According to Wei et. al. highest maximum power output is obtained from granular activated carbon compared to graphite and carbon felt anodes.[8]

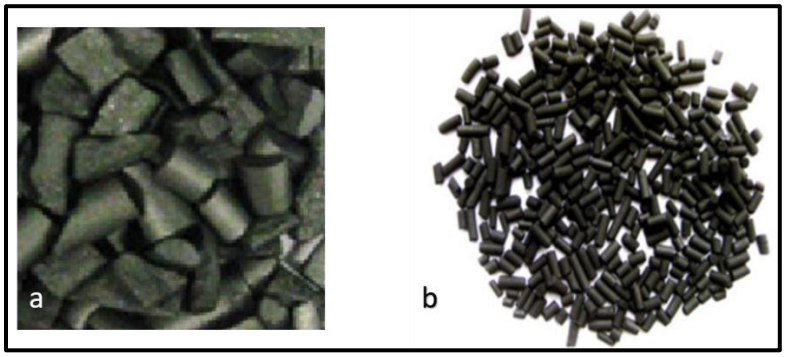

Figure 3.3(a) Granular graphite (b) Granular activated carbon

Brush structure:

Logan et al [5] reported graphite brush anode as an ideal electrode that can achieve efficient current collection and high surface area. According to their studies, "carbon fibre brushes of set length wound into a twisted core made up of titanium wires"[8]. But, some clattering was revealed in the brush configuration which prohibited the bacteria access and limited the contact between the microbes and the material, thus resulted in low power generation. Brush anodes are shown in figure 3.4.

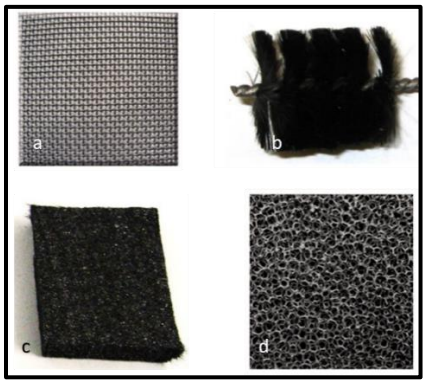

Figure 3.4 (a) Stainless Steel Mesh (b) Carbon Brush (c) Graphite felt (d) Reticulated vitrified carbon

3.3.2 Proton Exchange Membrane

Proton Exchange is a very important component of an MFC. It influences the electrochemical performance of an MFC. The structure of PEM enables only the transfer of protons and hydrogen ions through it. Nafion ionomer is the most widely used polyelectrolyte for proton exchange membrane due to its ability to increase the 3D zone of catalytic activity. “Hydrogen with proton exchange membrane fuel cells (PEMFCs) is currently considered as a potential next generation alternative energy technology because of the high energy density and high abundance of hydrogen in nature.” [11] Hydrogen ions pass through the PEM to either form water in the case when oxygen is the electron acceptor or form ferricyanide from ferrocyanide when ferricyanide is the electron acceptor and hence completing the circuit.

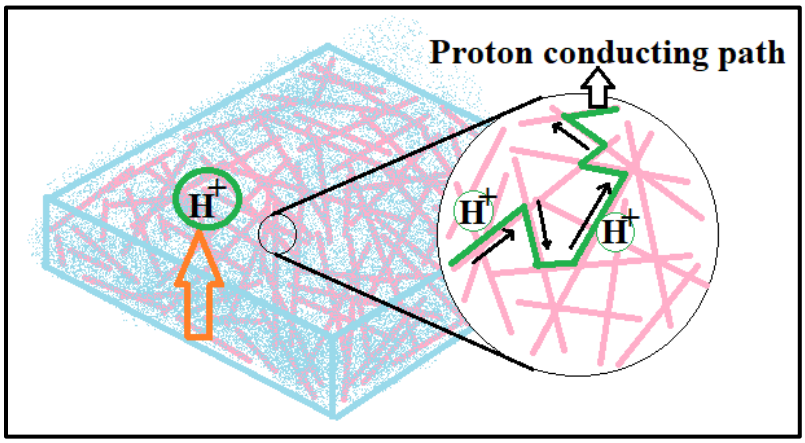

Figure 3.5 PEM structure allowing H^+ ions to pass through [12]

3.3.3 Exoelectrogenic Bacteria that power MFCs

The highest power densities in MFCs are almost always produced by inoculating the anode with a rich and diverse source of bacteria, such as a waste water or sludge. The power densities

produced by isolates or mixed cultures are often more dependent on the specific architecture, electrode spacing and solution conductivity of the fuel cell rather than the specific bacterium. Thus, power densities produced by a bacterium in one study cannot be directly compared with another bacterium or a mixed culture unless the MFC architecture and chemical solution are the same. In addition, the internal resistance of the device must be low to ensure that differences between different bacterial strains can be detected. Proof that a specific MFC will work in such a comparison can only be determined through extensive testing of different strains and inocula in the device. The low power densities obtained using various *Geobacter* strains in MFCs (7–45 mW per m^2) in early two-chamber MFC studies, for example, are now known to be due to the high internal resistance of these systems. The development of simple, single chamber designs with a lower internal resistance have allowed examination of a range of factors that affect power production, including the inoculum. With these reactors, a high power-producing bacterium, and the first Alphaproteobacterium to be isolated from an MFC, was shown to produce more power than a mixed culture. Based on the observation that MFCs inoculated with a waste-water sample often developed a bright red colour over time, which is a characteristic of purple sulphur and non-sulphur bacteria, the members of my laboratory plated and picked colonies that had an obvious red colour. one of these isolates, *R. palustris* DX-1, produced a maximum power density (2,720 mW per m^2) that was 56% larger than that produced by the original inoculum (1,740 mW per m^2) and 13% larger than that previously obtained in this device under similar conditions. The maximum power produced in a comparison of pure and mixed cultures is affected by electrode sizes and reactor architecture. using a single-chamber, air cathode MFC with a low internal resistance, it was shown that an enriched consortium of microorganisms produced 22% more power (576 mW per m^2) than a pure culture of *Geobacter sulfurreducens* (461 mW per m^2; normalized to cathode area; anode to cathode ratio of 1.5) despite the presence of *G. sulfurreducens* in the consortium. With

equally sized electrodes in another air cathode MFC, *G. sulfurreducens* produced 240 mW per m^2 (normalized to anode area) but power production was not compared with a mixed culture. When the anode size was reduced (anode to cathode ratio of 1:8), and ferricyanide was used as a catholyte instead of oxygen, *G. sulfurreducens* produced 19% more power (1.9 W per m^2) than a mixed culture (1.6 W per m^2). This different outcome in the complete absence of oxygen suggests that *G. sulfurreducens* is capable of producing high power densities if oxygen intrusion into the MFC (through the cathode) is avoided or perhaps if other microorganisms are present to scavenge the oxygen. *Shewanella putrefaciens* was first shown to produce electricity in the absence of exogenous mediators in 1999. The mechanism used by *Shewanella* spp. to transfer electrons outside the cell continues to be a subject of debate, perhaps owing to the fact that there may be no single answer. *Shewanella* spp. Have outer membrane cytochromes for direct electron transfer by contact, but they can also extrude electrically conductive nanowires. *S. oneidensis* also produces flavins that can function as electron shuttles. Despite the possibility that this bacterium could use multiple methods for exocellular electron transfer, *S. oneidensis* produced 56% less power than an acclimated waste-water inoculum in an air cathode MFC in fed batch tests. The reasons for these lower power densities could include ineffective interaction of electron-transferring molecules (cytochromes, flavins or those in nanowires) with the carbon electrode compared with a metal oxide. Redox conditions in fed batch MFCs fluctuate over a cycle (the time before current generation substantially decreases after the substrate is depleted), and variations from positive to negative redox potentials over a cycle may interfere with physiological optimization of power production. The production of high power densities has been shown to be possible by growing *Shewanella* cells under low oxygen conditions and then pumping the cell suspension through a small (1.2 ml) reactor with an air cathode (2 W per m^2 or 330 W per m^3) or ferricyanide cathode

(3 W per m^2 or 500 W per m^3). *Shewanella* spp. therefore seem to be inherently capable of high power densities under certain reactor conditions[13].

Year	Microorganism	Comment
1999	*Shewanella putrefaciens* IR-1 (REF. 30)	Direct proof of electrical current generation in an MFC by a dissimilatory metal-reducing bacterium (Gammaproteobacteria)
2001	*Clostridium butyricum* EG3	First Gram-positive bacterium shown to produce electrical current in an MFC (phylum Firmicutes)
2002	*Desulfuromonas acetoxidans*[51]	Identified in a sediment MFC community and shown to produce power (Deltaproteobacteria)
	Geobacter metallireducens[51]	Shown to generate electricity in a poised potential system (Deltaproteobacteria)
2003	*Geobacter sulfurreducens*[40]	Generated current without poised electrode (Deltaproteobacteria)
	Rhodoferax ferrireducens[24]	Used glucose (Betaproteobacteria)
	A3 (*Aeromonas hydrophila*)[52]	Deltaproteobacteria
2004	*Pseudomonas aeruginosa*[10]	Produced low amounts of power through mediators such as pyocyanin (Gammaproteobacteria)
	Desulfobulbus propionicus[53]	Deltaproteobacteria
2005	*Geopsychrobacter electrodiphilus*[30]	Psychrotolerant (Deltaproteobacteria)
	Geothrix fermentans	Produced an unidentified mediator (phylum Acidobacteria)
2006	*Shewanella oneidensis* DSP10 (REF. 33)	Achieved a high power density (2 W per m^2 or 500 W per m^3) by pumping cells grown in a flask into a small (1.2 mL) MFC (Gammaproteobacteria)
	S. oneidensis MR-1 (REF. 54)	Various mutants identified that increase current or lose the ability for current generation (Gammaproteobacteria)
	Escherichia coli[55]	Found to produce current after long acclimation times (Gammaproteobacteria)
2008	*Rhodopseudomonas palustris* DX-1 (REF. 37)	Produced high power densities of 2.72 W per m^2 compared with an acclimated waste-water inoculum (1.74 W per m^2) (Alphaproteobacteria)
	Ochrobactrum anthropi YZ-1 (REF. 11)	An opportunistic pathogen, such as *P. aeruginosa* (Alphaproteobacteria)
	Desulfovibrio desulfuricans[56]	Reduced sulphate when growing on lactate; resazurin in the medium was not thought to be a factor in power production (Deltaproteobacteria)
	Acidiphilium sp. 3.2Sup5 (REF. 57)	Current at low pH and in the presence of oxygen in a poised potential system (Alphaproteobacteria)
	Klebsiella pneumoniae L17‡ (REF. 58)	The first time this species produced current without a mediator (Gammaproteobacteria)
	Thermincola sp. strain JR[59]	Phylum Firmicutes
	Pichia anomala‡ (REF. 5)	Current generation by a yeast (kingdom Fungi).

Figure 3.6 Culture studies show exoelectrogenic activity without exogenous mediators[13]

3.4 MFC Design

3.4.1 Single-Chamber MFCs

Single-Chamber MFCs are one-compartment MFCs which do not have a cathodic chamber due to the exposure of cathode directly to the air. The most common design of such MFC is the cube reactor design as shown in Figure 3.6.

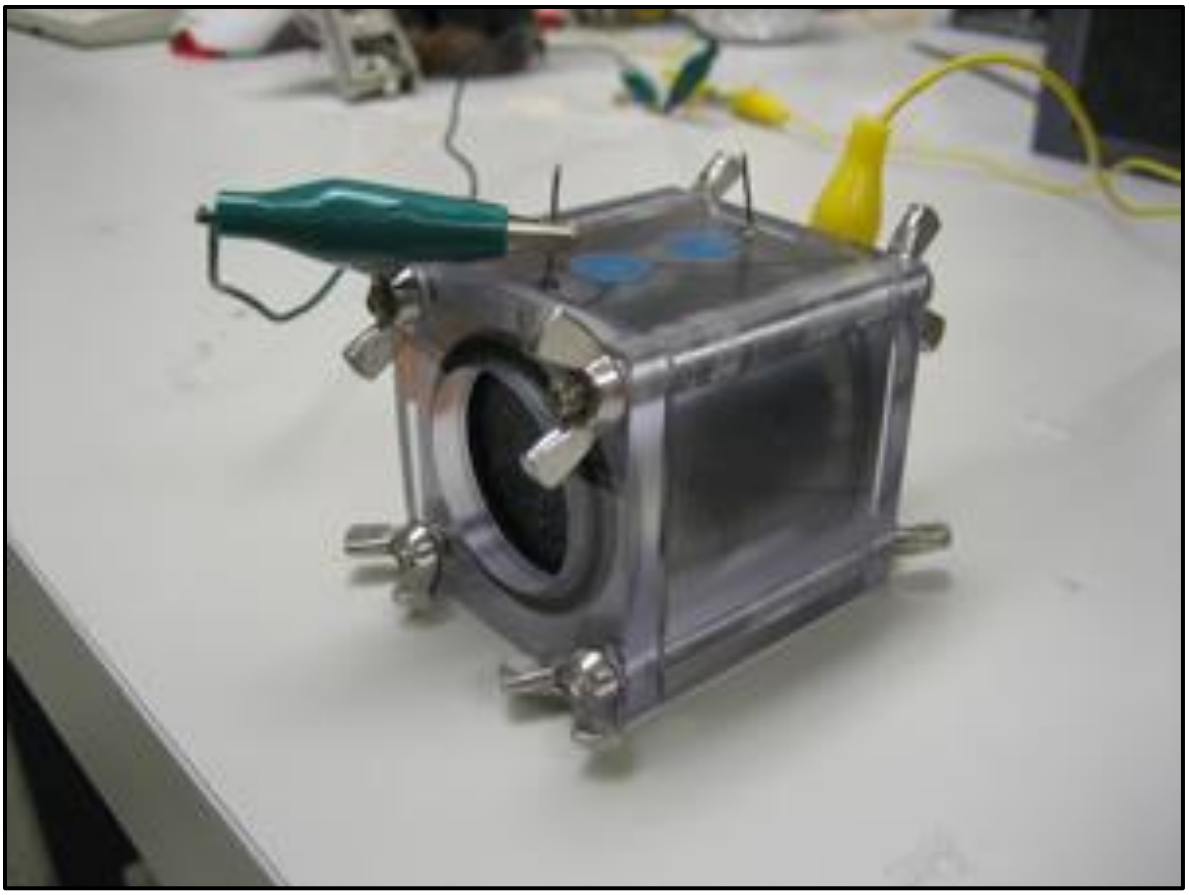

Figure 3.7 Single Chamber MFC (Logan et al 2007)

The single-chamber MFC consists of an anode in a rectangular anode chamber coupled with air-cathode. Protons are transferred from the anolyte solution to the porous air –cathode. Material used in cube is Perspex plastic. [1]

3.4.2 Double-Chamber MFCs

Double-chamber MFC configuration or H-shaped MFC configuration is the most widely used MFC configuration having two compartments containing anode, anolyte and cathode, catholyte separated by a proton exchange membrane(PEM). (Figure 3.1). Since most of the microbes used in MFCs are anaerobic in nature therefore, the anode chamber is kept free of oxygen for anaerobic breakdown process to occur,by purging with nitrogen. Although the H-shaped MFC is most commonly used in the laboratory but scaling it up is very difficult due to the impractical configuration. The single-chamber MFC is easiest to scale-up as it uses air directly as an oxygen source and also due to its low material usage resulting in overall low cost. Figure 3.7 is a basic schematic of a dual chambered MFC. [1]

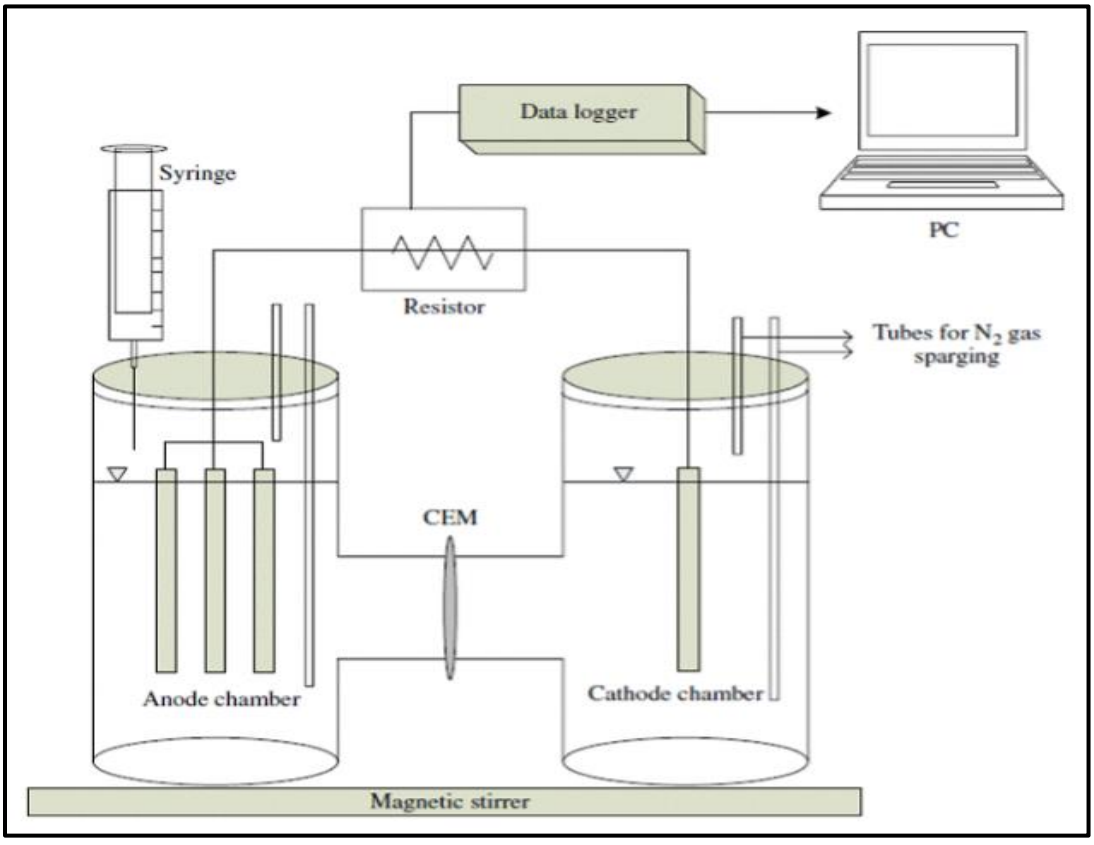

Figure 3.8 H-shaped double-chambered MFC in batch operation mode[1]

This set up can house various electrode shapes, i.e. granular, plane and brush as it has a seperate chambers for the cathode and anode. Catholytes can be changed by their ability to accept electrons. It can also use other catholyte besides air, which is any source of oxygen. According to a recent research document, use of algae (seaweed) enhances the oxygen production due to photosynthetic process in the plant which can be facilitated by this type of MFC configuration. [14]

3.4.3 Tubular MFCs

The single-chambered, tubular, continuous microbial fuel cell uses granular graphite matrix as the anode which generates high power outputs. This type of MFC have proven to be most effective in continuous flow operation, however, there is about 57% change in the chemical oxygen demand concentration across the reactor and a significant decrease in current density. In an experiment conducted by Scott et al, using manure as the organic fuel source, carbon cloth as the electrodes and with no proton exchange membrane. This set up did not require a strictly controlled anaerobic environment and adapted the form of a helix which allows the fuel to flow through at a certain flow rate. [15] This MFC configuration is most applicable in commercial use as it yields high power densities with minimum cost in terms of the materials used. The coiled helix tubular MFC concept might be the next step to realising practical applications. Figure 3.8 shows the tubular model shows tubular MFC set up.

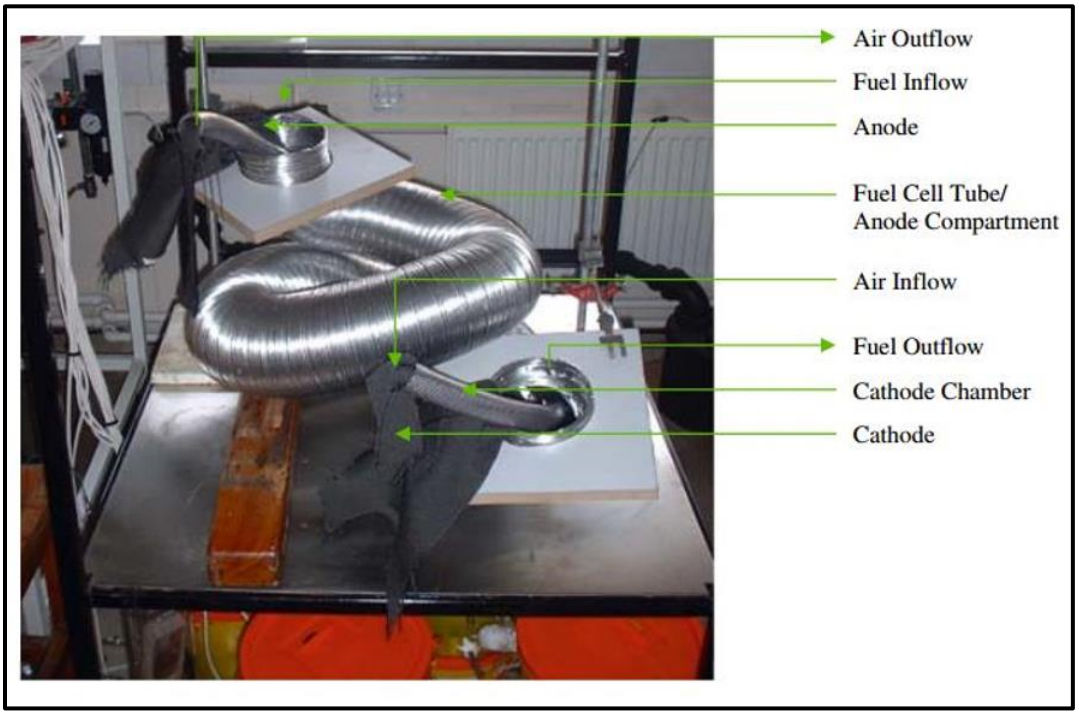

Figure 3.9 Coiled-helix tubular MFC setup

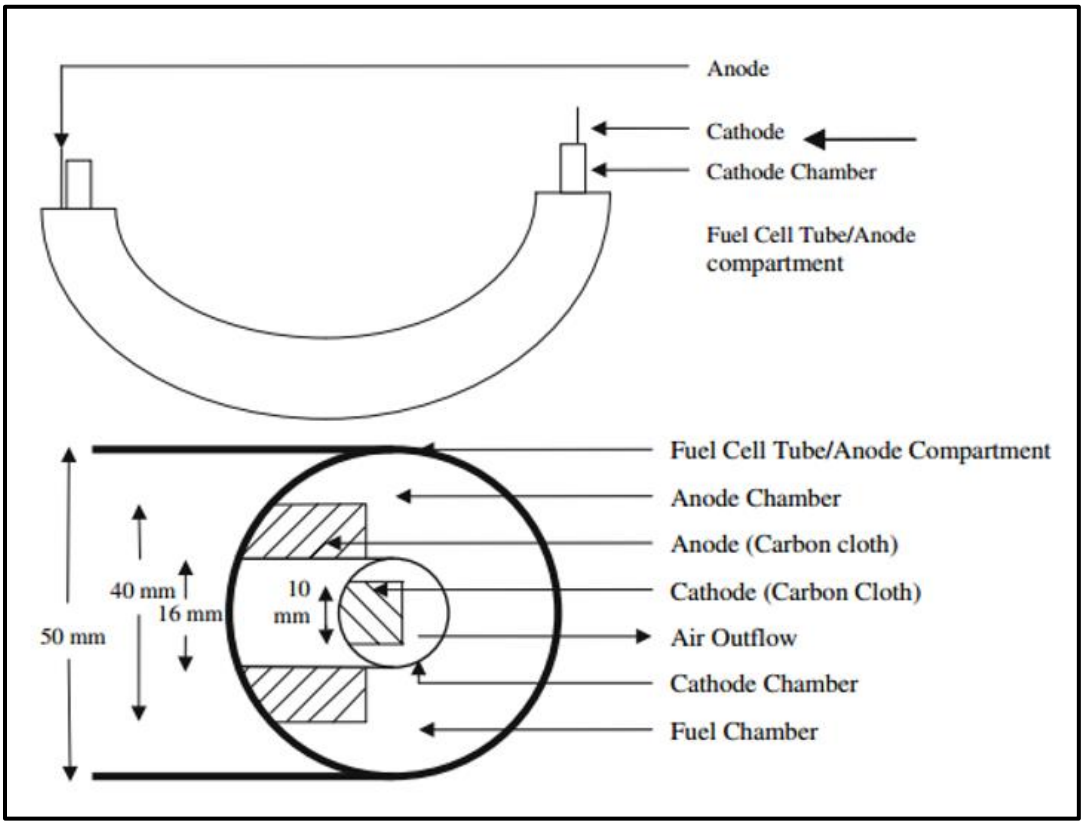

Figure 3.10 Schematic of tubular MFC

3.5 Potential Applications of MFC

3.5.1 Wastewater treatment plant

Clean water and electricity are essential in everyday life, but we often need one to get the other. Electricity generation is needed to purify water and we use water (hydro-generation) to produce energy. A significant fraction of the electricity generated is used to power the water infrastructure. MFC technology possesses the potential to address this issue as it is able to extract electricity directly from the wastewater using the various bacteria within the wastewater. Bacteria contained in the wastewater, thought of previously as the biggest challenge in generating large power outputs. However, it is everything but the bacteria that is the greatest problem. The challenge predominantly lies in the engineering large scale MFCs to accommodate large quantities of wastewater (e.g. 10,000 l) The hope in the future is that wastewater treatment plants which consume electricity to power plants generating electricity.

"Electricity produced by MFCs may never be a cost effective source of energy in its own right. Rather their contribution will be one of reducing the energy used in wastewater treatment."[7] Wastewater treatment systems consists of a series of unit processes each having specific functions which contributes to purifying the influent as it passes through the different stages. One of the stages involves aerobic biological processes which require both oxygen and food in order for the bacteria to live. The bacteria consume biodegradable soluble organic contaminants.

A power management system (PMS) is proposed as a method of increasing the power output by use of transformers, capacitors and converters. Zhang et al conducted tests to evaluate the feasibility of charge pump-capacitor-converter and capacitor-transformer-converter PMSs which yielded promising results. A sample of the various set-up used is shown in Figure 3.10. [16]

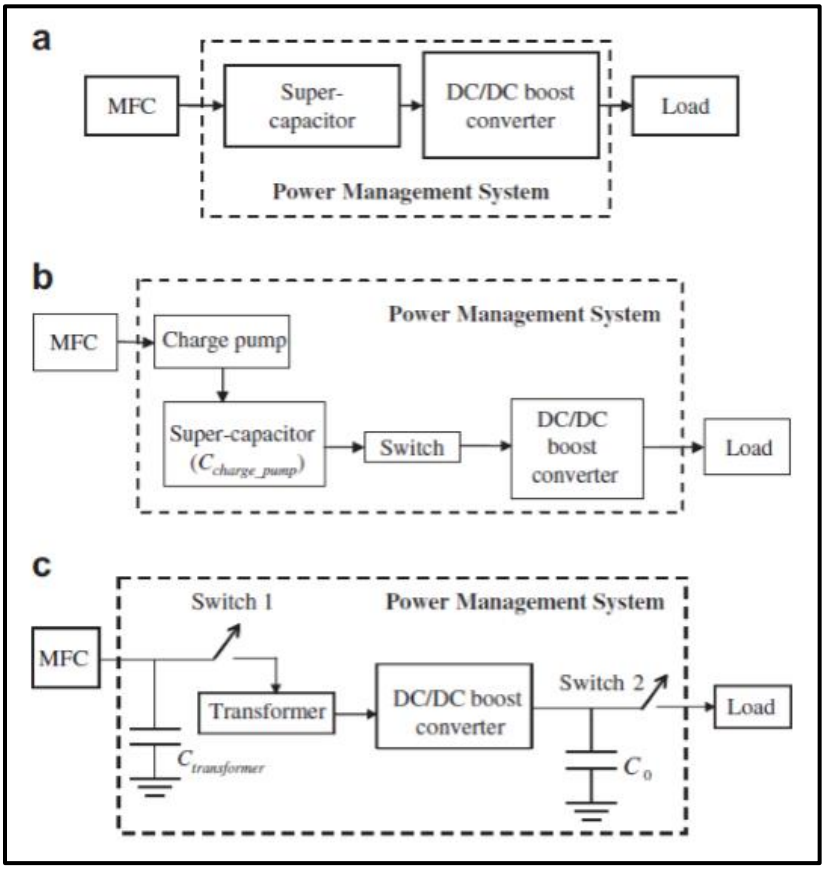

Figure 3.11 Basic schematics of different MFC PMSs (a) capacitor-converter type (b) charge pump-capacitor-converter type and (c) capacitor-transformer-converter type

According to Logan et al, aerobic wastewater treatment process takes up about 50% of the energy used in activated sludge processes which is approximately 0.6kWh for each cubic meter of wastewater. MFCs have shown to successfully treat wastewater which include domestic, animal, brewery and food processing wastewaters and generate current in the process. [17] However, the treatment is not as effective as the aerobic one and will require further treatment; this renders the MFC redundant as more energy will have to come elsewhere.

Using domestic wastewater as fuel source, an experiment conducted by Rodrigo et al reported that using anaerobic pre-treatment of activated sludge; electricity generation can be obtained in a short time period (8-10 days). The oxygen used is very small (only 0.25% of the influent chemical

oxygen demand (COD)) for electricity-generation processes. The max power densities is aroun 25mW/m^2 with a voltage of 0.23V using domestic wastewater. A MFC schematic is outlined in Figure 3.11. [18]

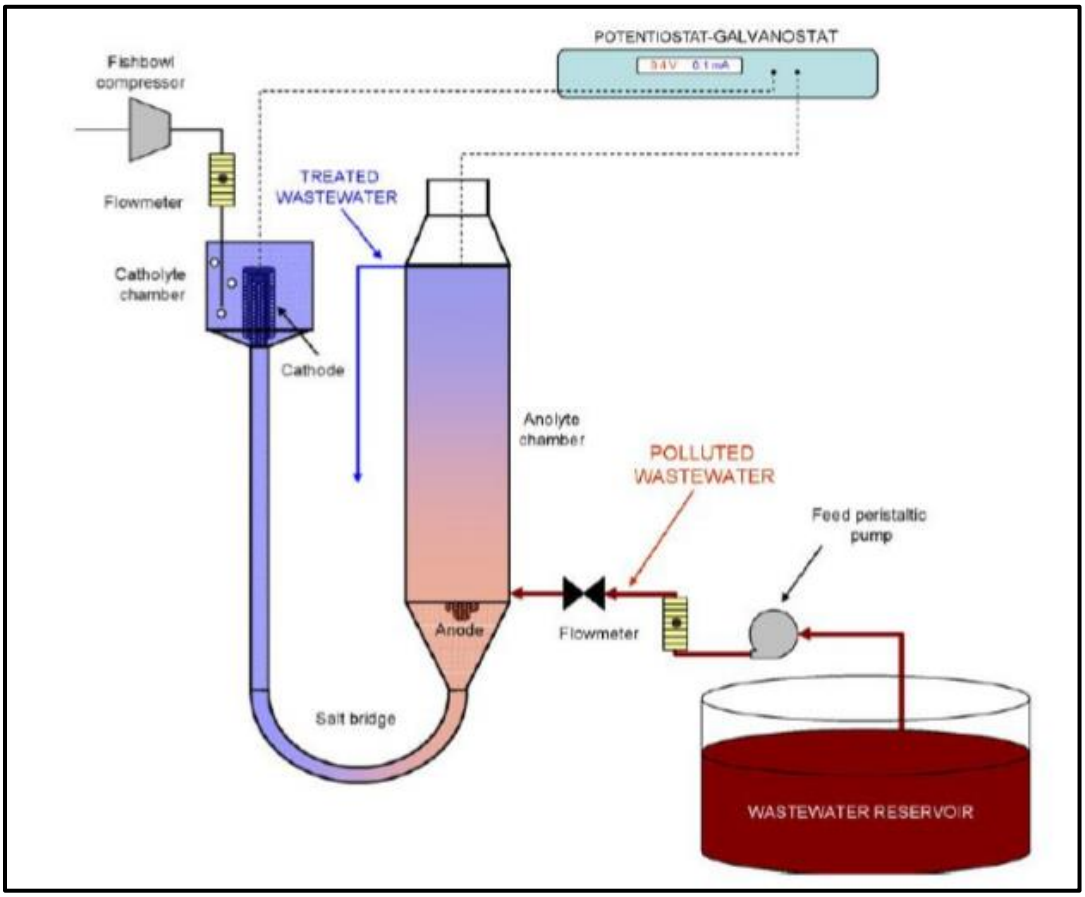

Figure 3.12 A continuous flow MFC set-up using domestic wastewater.[18]

MFCs in wastewater treatment processes are not only useful in treating wastewater using bacteria but can also generate electricity to power small sensors or offset power consumption overall.

3.5.2 To power various electrical devices, medical devices and biosensors

The principle of BioCapacitor

A BioCapacitor is composed of three main elements, as shown in Figure. The first element is an enzyme fuel cell, in which enzymes oxidize or reduce the substrate to generate electric power.

The second element is a charge pump circuit that boosts the voltage supply from the enzyme fuel cells.The third element is a capacitor that stores the boosted electric power. Using the BioCapacitor, sufficient electric power for operating electric devices can be generated without modifying the design and construction of the enzyme fuel cells. The BioCapacitor completes repeat charge or discharge cycles to supply sufficient electric power to electric devices as follow.

(1) With the supply of electric power from the enzyme fuel cells, the charge pump circuit is driven.

(2) The power is converted to the stepped-up electric power in the charge pump circuit.

(3) The stepped-up electric power output from the charge pump circuit is gradually charged to the capacitor until the voltage reaches the discharge start voltage.

(4) The comparator in the charge pump circuit compares the capacitor voltage with the discharge start voltage and outputs the digital signal indicating which is larger. When the capacitor voltage exceeds the discharge start voltage, discharge control switch turns on by the output signal of the comparator. As a result, the charge pump circuit switches from the charge step to the discharge step.

(5) Electric power is supplied to the electric device from the capacitor.

(6) The comparator in the charge pump circuit compares the capacitor voltage with the discharge stop voltage. When the capacitor voltage declines in the discharge stop voltage, discharge control switch turns off. As a result, the charge pump circuit switches to the charge step. Higher electricity-generating power results in short charge or discharge intervals in the BioCapacitor, Conversely, lower electricity-generating power results in long charge or discharge intervals. As the electricity-generating power of the enzyme fuel cells is dependent on the fuel concentration, the charge or dis- charge frequency of the BioCapacitor is dependent on the fuel concentration. In other words, the fuel concentration can be measured

using the charge or discharge frequency as an index. Additionally, the charge or discharge frequency also depends on the capacitance of the capacitor. A larger capacitance leads to longer charge or discharge intervals and the discharge of larger quantities of electricity at a time. [19]

Koji Sode et. al used a commercially available charging pump integrated circuit (IC) in which operation minimum input voltage and discharge start voltage are 0.3 and 1.8 V, respectively, to construct the BioCapacitor.

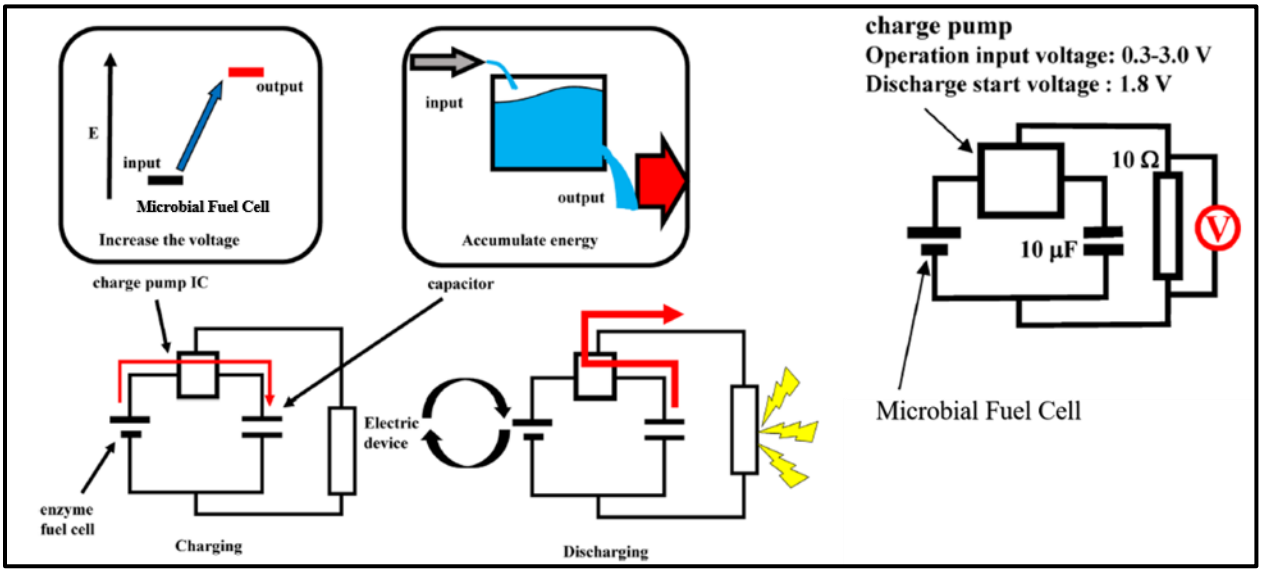

Figure 3.13 Using Charge pump to charge a capacitor from MFC in order to use it in different electrical and electronic devices

These advanced biofuel cell technologies and improvements of charge pump circuit performance will further expand the possibilities of the application of BioCapacitor principle in future stand- alone, self-powered, autonomous biodevices. Possibly, micro- processors will also be operated by the BioCapacitor principle, which is the necessary component for programmable

autonomous biodevices to operate self-powered sensor-based autonomous drug delivery systems, represented by the closed loop insulin pump system, to realize the artificial pancreas.[19]

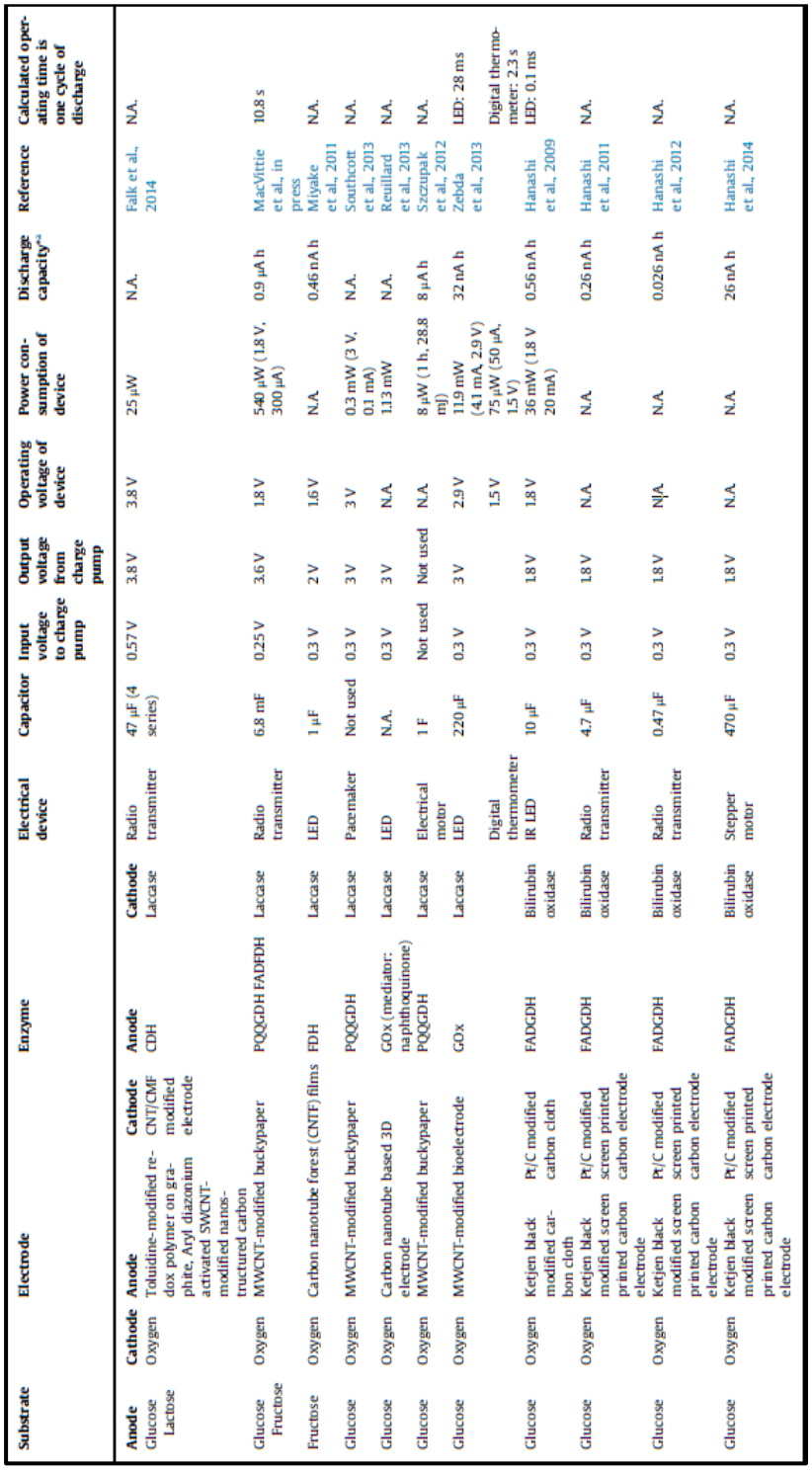

Substrate	Electrode		Enzyme		Electrical device	Capacitor	Input voltage to charge pump	Output voltage from charge pump	Operating voltage of device	Power consumption of device	Discharge capacity[a]	Reference	Calculated operating time is one cycle of discharge
Anode	**Cathode**	**Anode**	**Cathode**	**Anode**	**Cathode**								
Glucose Lactose	Oxygen	Toluidine-modified redox polymer on graphite, Aryl diazonium activated SWCNT-modified nanostructured carbon	CNT/CMF modified electrode	CDH	Laccase	Radio transmitter	47 μF (4 series)	0.57 V	3.8 V	3.8 V	25 μW	N.A.	Falk et al., 2014	N.A.
Glucose Fructose	Oxygen	MWCNT-modified buckypaper		PQQGDH FADFDH	Laccase	Radio transmitter	6.8 mF	0.25 V	3.6 V	1.8 V	540 μW (1.8 V, 300 μA)	0.9 μA h	MacVittie et al., in press	10.8 s
Fructose	Oxygen	Carbon nanotube forest (CNTF) films		FDH	Laccase	LED	1 μF	0.3 V	2 V	1.6 V	N.A.	0.46 nA h	Miyake et al., 2011	N.A.
Glucose	Oxygen	MWCNT-modified buckypaper		PQQGDH	Laccase	Pacemaker	Not used	0.3 V	3 V	3 V	0.3 mW (3 V, 0.1 mA)	N.A.	Southcott et al., 2013	N.A.
Glucose	Oxygen	Carbon nanotube based 3D electrode		GOx (mediator: naphthoquinone)	Laccase	LED	N.A.	0.3 V	3 V	N.A.	1.13 mW	N.A.	Reuillard et al., 2013	N.A.
Glucose	Oxygen	MWCNT-modified buckypaper		PQQGDH	Laccase	Electrical motor	1 F	Not used	Not used	N.A.	8 μW (1 h, 28.8 mJ)	8 μA h	Szczupak et al., 2012	N.A.
Glucose	Oxygen	MWCNT-modified bioelectrode		GOx	Laccase	LED	220 μF	0.3 V	3 V	2.9 V	11.9 mW (4.1 mA, 2.9 V)	32 nA h	Zebda et al., 2013	LED: 28 ms
						Digital thermometer				1.5 V	75 μW (50 μA, 1.5 V)			Digital thermometer: 2.3 s
Glucose	Oxygen	Ketjen black modified carbon cloth	Pt/C modified carbon cloth	FADGDH	Bilirubin oxidase	IR LED	10 μF	0.3 V	1.8 V	1.8 V	36 mW (1.8 V 20 mA)	0.56 nA h	Hanashi et al., 2009	LED: 0.1 ms
Glucose	Oxygen	Ketjen black modified screen printed carbon electrode	Pt/C modified screen printed carbon electrode	FADGDH	Bilirubin oxidase	Radio transmitter	4.7 μF	0.3 V	1.8 V	N.A.	N.A.	0.26 nA h	Hanashi et al., 2011	N.A.
Glucose	Oxygen	Ketjen black modified screen printed carbon electrode	Pt/C modified screen printed carbon electrode	FADGDH	Bilirubin oxidase	Radio transmitter	0.47 μF	0.3 V	1.8 V	N/A	N.A.	0.026 nA h	Hanashi et al., 2012	N.A.
Glucose	Oxygen	Ketjen black modified screen printed carbon electrode	Pt/C modified screen printed carbon electrode	FADGDH	Bilirubin oxidase	Stepper motor	470 μF	0.3 V	1.8 V	N.A.	N.A.	26 nA h	Hanashi et al., 2014	N.A.

Figure 3.14 Use of biocapacitor concept on different electrical devices

CHAPTER-4

4. Materials and Methods

4.1 Chemicals and reagents:

An aluminium sheet (0.143 mm thick), Wax, Whatman filter paper grade 1, Natural Graphite flakes (Sigma-Aldrich), Graphite paste, Agar extra pure (alfa aesar) and KCl purified (lobachemie) were used for fabrication of miniaturised MFC. Sodium phosphate monobasic (Sisco Research Laboratories), disodium hydrogen phosphate dihydrate (Merck), NaCl (Sisco research laboratories), potassium ferricyanide (Merck) and potassium ferrocyanide (Merck) were used for the preparation of Phosphate Buffered Saline Ferro-Ferri (PBS Ferro-Ferri solution). Sodium carboxymethyl cellulose (Rankem), $MnCl_2$ (CDH), $CaCl_2$ (Avarice), Dipotassium Hydrogen orthophosphate (CDH), Potassium dihydrogen orthophosphate (CDH), Sodium fluoride (CDH), Sorbitol (CDH), Methyl-p-hydroxybenzoate (CDH) were used for preparation of artificial saliva. Ethylcarbodiimide hydrochloride (EDC) was obtained from Sigma-Aldrich and N-hydroxysulfosuccinimide (NHS) was purchased from Fischer scientific. Glutaraldehyde solution 25% was purchased from Merck for fixing the biological samples for Scanning Electron Microscopy. All the chemicals were of analytical grade and were used without further purification. 50 mM phosphate buffer saline (PBS) solution of pH 7.0 was prepared by dissolving sodium phosphate monobasic, di-sodium hydrogen phosphate dihydrate and 0.9 % NaCl in Milli-Q water having resistivity of 18 MΩ cm and stored at 4°C. Thus, freshly prepared PBS solution was used for performing all electrochemical studies as well as used as a catholyte. α-amylase and lysozyme were purchased from Sigma-Aldrich. These biomolecules were diluted to the desired concentration using deionized water having pH 7 and stored at -20°C until further use.

4.2 Fabrication of double-chambered Microbial Fuel Cell (MFC)

Double chambered MFC was fabricated using two 100 mL sterilised plastic containers, 15 mL centrifuge tube, copper wire for connecting the anode and cathode, and glue gun to seal the resulting H shape MFC formed. Freshly made gel for proton exchange membrane (PEM) containing 5% agarose and 2.5% KCl was poured inside the 15 mL centrifuge tube and 4 cm of it was cut to be inserted inside the H-shaped MFC. After inserting inside the plastic containers the H-shaped structure was sealed using glue gun so that no leakage occurs. Electrodes of dimension 2 cm by 3 cm were prepared using aluminium foil coated with graphite paste on both sides and other electrode materials like polyaniline, rGO etc. After preparing the electrodes, they were inserted inside the MFC in the anode and cathode chambers and were given connection to the load via copper wires. Anolyte (Rotten potato paste) and catholyte (Phosphate Buffered Saline ferro-ferri pH 7) were added to both chambers and the resulting readings were taken.

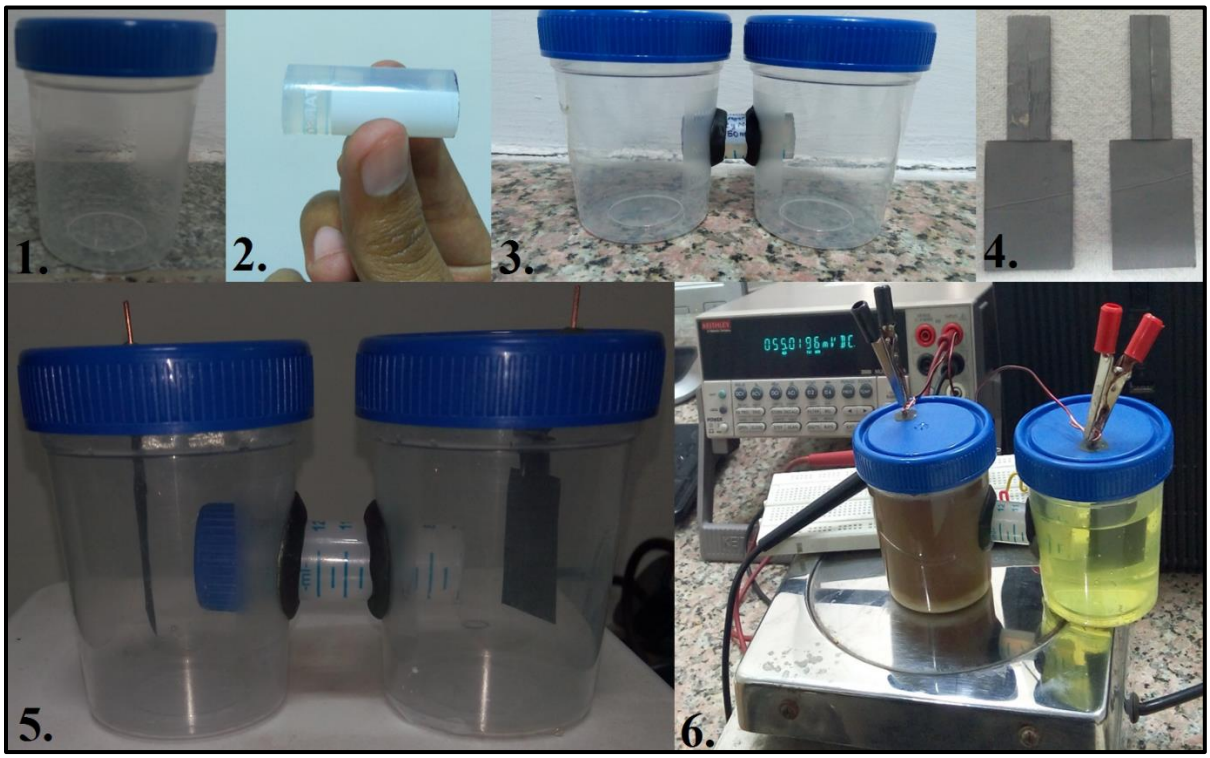

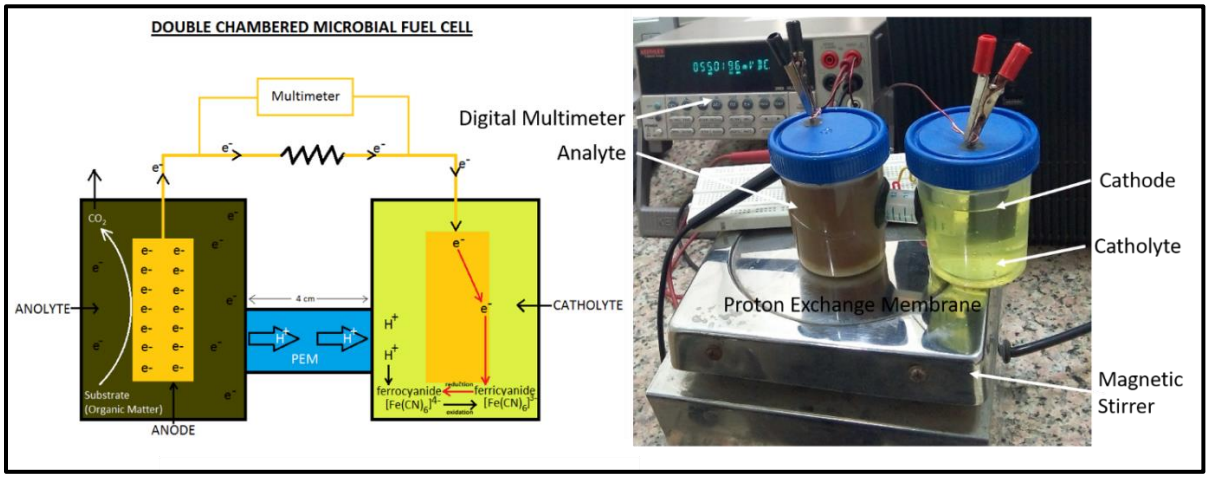

Figure 4.1 Fabrication process of double-chambered MFC and its components

4.3 Fabrication of Miniaturized Microbial Fuel Cell

Aluminium sheet was cut into a square having side of length 4 cm and having a contact of 3 cm length and 1 cm breadth on one of its side. Another square having a side of length 3 cm was marked inside the previous square and was perforated several times with the help of a sharp nail as shown in the figure. After this double sided tape was used to cover the remaining plain surface of the aluminium sheet on both upper as well as the lower surface. Now, graphite paste was poured in the well created by the use of double-sided tape. Once the well was completely filled Whatman filter paper was cut into squares having sides 3 cm and 4 cm. The first square having side 3 cm was placed above the graphite paste and then the bigger square having side of 4 cm was placed over the electrode after removing the protective layer from the double sided tape. Similarly, another electrode was prepared and was left to dry in hot air oven at a temperature of 60°C. After this process, the sides of the resulting electrodes were made hydrophobic up to a length of 0.5 cm from the outer side on all sides using melted wax.

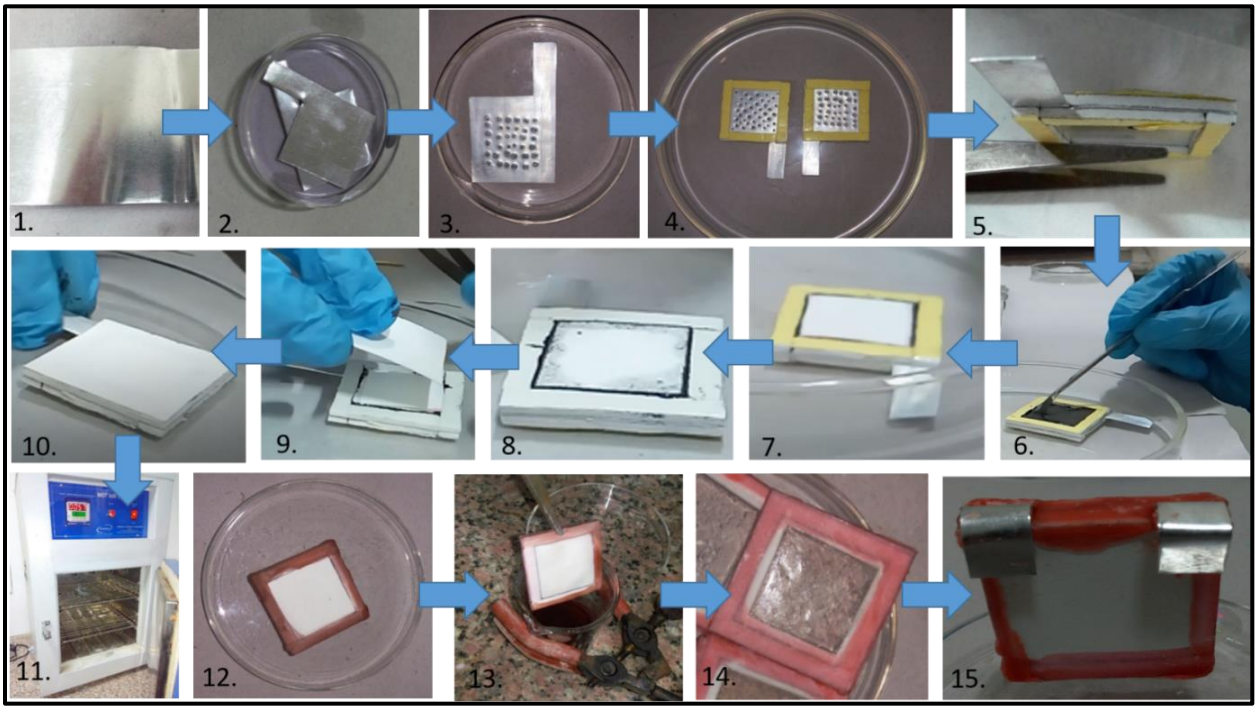

Figure 4.2 Steps for fabrication of miniaturized MFC to power biosensors

Proton Exchange Membrane was prepared using a Whatman filter paper cut into a square having side 4 cm. Outer 0.5 cm of this paper was made hydrophobic using wax. After this, a solution containing 5% agar and 2.5% KCl was prepared by heating at 75°C and is then poured on the hydrophilic surface of Whatman filter paper square prepared. Immediately after pouring glass was used to evenly distribute agar gel over the paper surface and the same process was repeated on the other side of the proton exchange membrane to be prepared.

Miniaturized MFC was assembled using wax as shown in the figure above[20]. The temperature for wax coating was needed to be optimized as wax having high temperature could increase the area of the hydrophobic surface. The sole purpose of using wax was to provide a hydrophobic surface and also provide a support structure to MFC prepared. The MFC fabricated was then used for further experiments.

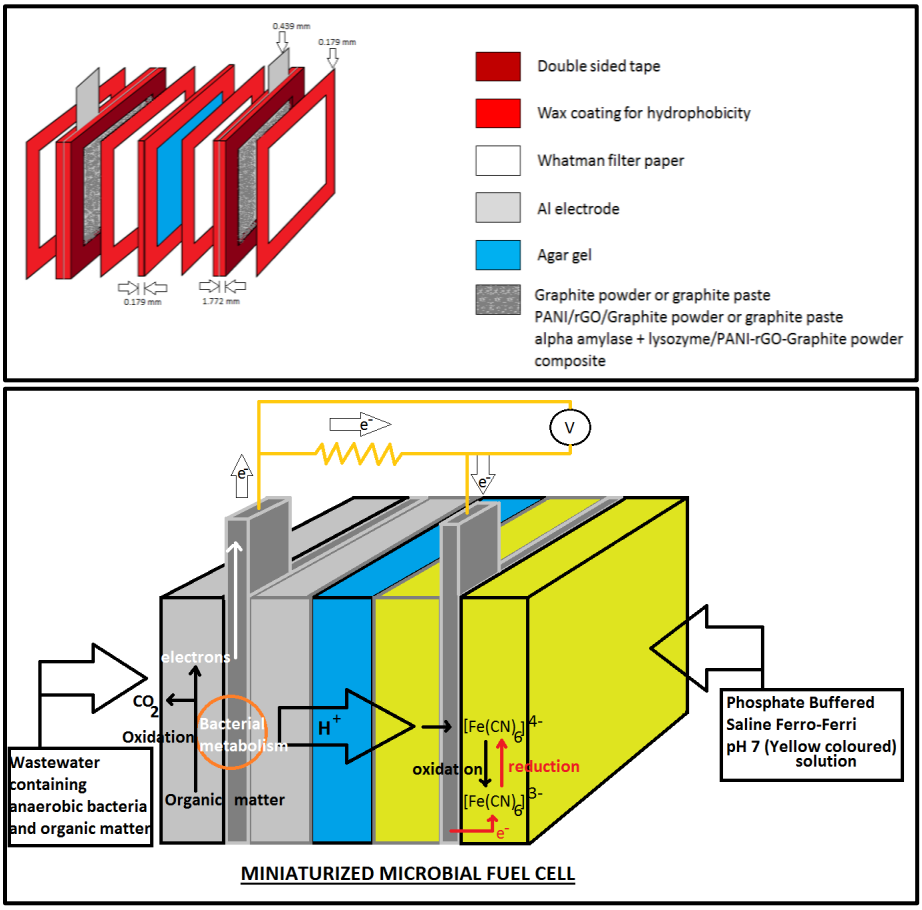

Figure 4.3 Fully assembled miniaturized MFC

Anolyte and Catholyte

Rotten potato mesh dissolved in equal volume of deionized water and the starch solution was taken as anolyte while a phosphate buffered saline ferrocyanide-ferricyanide solution (50 mM pH 7.0) was used as the catholyte. The presence of a good electron acceptor in the catholyte has an equal effect on the electricity produced by the MFC. Ferricyanide solution was used instead of oxygen because oxygen may penetrate the PEM to reach the anolyte where its presence may lead to changes in the metabolic pathways of anaerobic bacteria. Another reason being the level of difficulty in providing oxygen to the catholyte. The role of ferrocyanide ions is to accept the protons coming from the anode chamber to form ferricyanide ions which have a role as an electron acceptor. Anolyte and catholyte were introduced into the MFC chambers by pipetting 2mL on each side in case of miniaturized MFC[20].

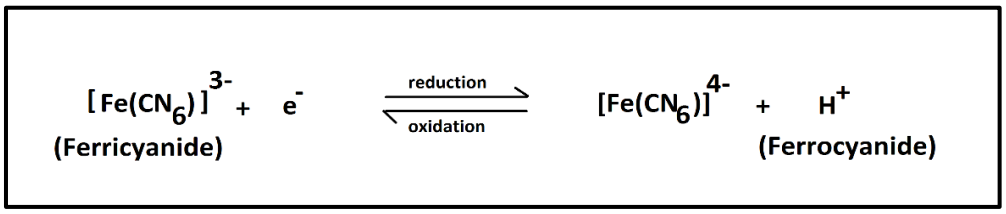

Figure 4.4 Reactions in catholyte of MFC

Immobilization of enzymes

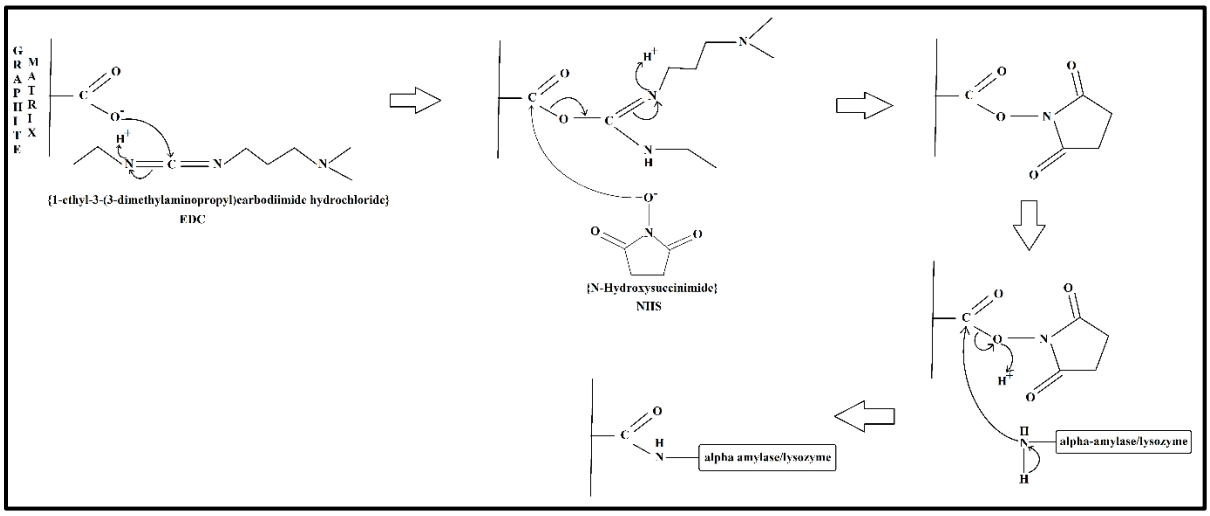

Figure 4.5 Crosslinking of Enzymes with the help of EDC and NHS

We used Lysozyme and α amylase. α amylase hydrolyzes alpha bonds of alpha-linked polysaccharides like starch present in potato to glucose and maltose which could be used by exoelectrogens as a food source. This will lead to the higher growth of bacteria present in rotten potato paste. Lysozyme catalyzes the hydrolysis of 1,4-beta-linkages between N-acetylmuramic acid and N-acetyl-D-glucosamine residues in peptidoglycan, which is the major component of gram-positive bacterial cell wall causing lysis of the bacteria. Due to the lysis of bacterial cell wall, the electrons present inside the bacteria would be released causing an abrupt increase in the current value from an MFC. Enzymes α amylase and lysozyme were immobilized on anode surface

with the help of crosslinkers like EDC (1-ethyl-3-(3 dimethyl aminopropyl)carbodiimide hydrochloride) and NHS (N-hydroxysuccinimide).

Figure 4.5 explains the mechanism for crosslinking of enzymes on graphite electrode surface.

For efficient immobilization of enzymes on 9 cm^2 anode area, 90 µL of 0.4 M EDC was first mixed with 90 µL of 0.1 M NHS in a microfuge tube and left for incubation for 10 minutes. After this step 90 µL of α amylase and 90 µL of lysozyme was added to the same microfuge tube and left for incubation for 20 minutes. The resulting 360 µL of the sample prepared was pipetted into anode surface and left overnight for efficient immobilization. Next day the anode surface was washed with PBS buffer in order to remove unbound enzymes.

4.4 Instrumentation:

4.4.1 Scanning electron microscopy:

A scanning electron microscope is used to study the surface morphology (shape, size) and topography (surface features) of nanomaterials. In this, electron beams (20-30 KeV) are used to determine the surface morphology by generating a magnified image on a very fine scale (10x to 500,000x). During scanning, electrons interact with the surface being imaged, leading to the generation of secondary electrons and back scattered electrons. Secondary electrons determine the morphology and topography of sample being scanned while contrast is being determined by back scattered electrons. SEM studies have been carried out using Hitachi S-3700N. In this work, SEM has been used for morphological analysis of electrodes prepared to be used in miniaturized MFC in order to confirm the growth of microbes as well the surface morphology of electrode surface.

Figure 4.6 Scanning Electron Microscope (Hitachi S-3700N)

Bacterial fixation and imaging

After all the readings were taken, the MFC was disassembled a minute portion of the anode was cut and the bacteria present in it were fixed with 2.5% glutaraldehyde solution overnight at 4°C. Samples were then dehydrated by 10, 30, 50, 70, 90 and 100 % ethanol. Fixed samples were examined using Scanning Electron Microscopy.

4.4.2 Transmission electron microscopy:

It is a microscopic technique in which a beam of accelerated electrons passes through an ultra-thin specimen (less than 200 nm) for the interaction with the sample with the help of condenser lens system. The interaction of electron beam and sample results in image formation which is further focussed and magnified on imaging device detected by the CCD camera. TEM provide high-resolution images (ranging from 50 to 10^6) than the light microscope. TEM is commonly operated in Bright Field (BF) imaging mode. In BF mode the contrast formed directly by absorption and occlusion of electrons in the sample. Sample regions with thickness or higher atomic number will appear dark and the region with no sample will appear bright. In this work, we have used TEM for characterization of electrode material used in MFC with and without microbes.

Precautions:

(i) The solvent used should not interact with the sample used.

(ii) The energy of the electron beam should be optimised as per the need of the sample.

4.4.3 UV/Vis/NIR Spectroscopy:

When a sample is exposed to light wave having energy that matches the energy difference between a possible electronic transition within the molecule, a fraction of the light energy would be absorbed by the molecule and the electrons would be shifted to the higher energy state orbital. A spectrometer registers the degree of absorption of light energy by a sample at different wavelengths and the resulting plot of absorbance (A) versus wavelength (λ) is known as a spectrum.

Beer's Law

"The intensity of a beam of monochromatic light decrease exponentially with the increase in the concentration of the absorbing substance".

Arithematically;

$$\frac{-dI}{dc} \propto \mathrm{I}$$

$$I = I_0 e^{-kc} \quad \text{... Eq. (4.1)}$$

Lambert's Law

"When a beam of light is allowed to pass through a transparent medium, the rate of decrease of intensity with the thickness of medium is directly proportional to the intensity of the light"

Mathematically;

$$\frac{-dI}{dt} \propto I$$

$$\ln I = kt + b \quad \text{... Eq. (4.2)}$$

Combination of the above two equations gives,

$$A = Kct \quad \text{... Eq. (4.3)}$$

Above equation is Beer's Lambert law.

Absorption spectra of any radiation arise from transition of an electron within a molecule from a lower energy level to a higher energy level. A molecule absorbs ultraviolet radiation of frequency (υ), the electron in that molecule undergo a transition from lower to higher energy level. The energy can be calculated by the equation,

$$E_1 - E_0 = h\upsilon \quad \text{... Eq. (4.4)}$$

Components of spectrophotometer:

- Source
- Monochromator

- Sample compartment
- Detector
- Recorder

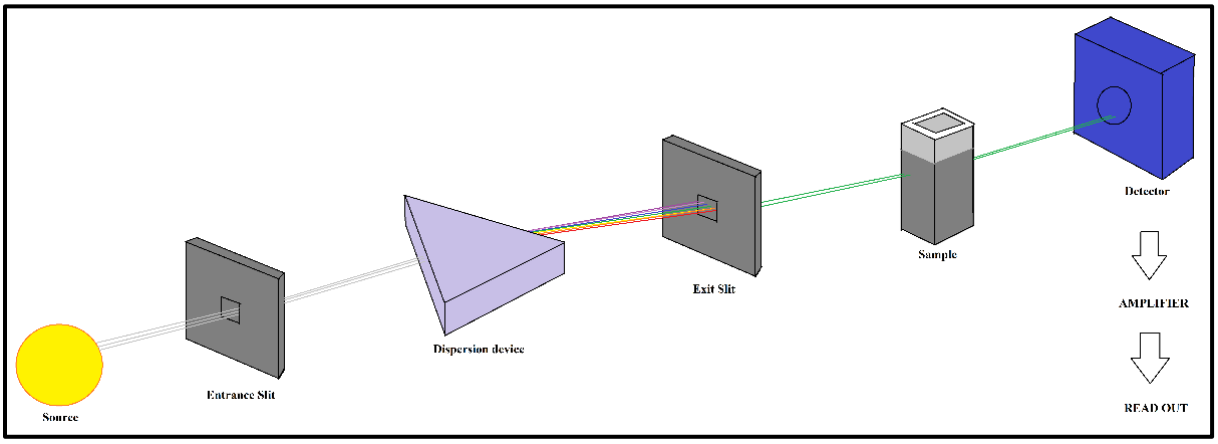

Figure 4.7(a) Working principle of UV/Vis/NIR Spectrophotometer

Figure 4.7(b) UV/Vis/NIR Spectrophotometer (Perkin Elmer Lambda 950)

Perkin Elmer Lambda 950 UV/Vis/NIR spectrophotometer was used to measure the optical density of microbial culture used in MFC in order to find the growth of same microbes in different electrode materials. Optical density was measured at a wavelength of 546 nm.

4.4.4 Electrochemical Techniques

Electrochemical techniques relate the changes of an electrical signal to an electrochemical signal at an electrode surface, usually as a result of an imposed potential or current. In a solution, the equilibrium concentrations of the reduced and oxidised forms of a redox couple are linked to the potential (E) via the **Nernst's Equation**

$$E = E_0 + \frac{RT}{nF} \ln \frac{C_{oxi}}{C_{red}} \quad \text{... Eq. (4.5)}$$

Where E_0 is equilibrium potential, F is Faraday's constant, T is absolute temperature, C_{ox} and C_{red} are concentrations of oxidation and reduction centres. If the potential E is applied to the working electrode with respect to the reference electrode e.g. via Potentiostat, the redox couples present at the electrode respond to this change and adjust their concentration ratios according to Eq. above. The figure shows electrochemical analyzer (Autolab Potentiostat/Galvanostat, Netherland, Cyclic Voltammetry (CV), differential pulse voltammetry (DPV), electrochemical impedance spectroscopy (EIS) are widely used electrochemical techniques. In this work CV has been performed for different electrode materials used in MFC and EIS has been performed to measure the internal resistance of miniaturised MFC.

CV (Cyclic voltammetry) studies were conducted to characterize the fabricated electrodes viz. bare Al, bare Graphite paste, Graphite paste/Al, PANI/Graphite paste/Al, rGO/Graphite paste/Al and PANI/rGO/Graphite paste/Al electrodes in a potential range from -0.8 to 0.8 V and scan rate of 0.050 V/s using 0.05 M PBS solution containing 5×10^{-3} M $[Fe(CN)_6]^{3-/4-}$.

Ideal capacitor follows the following relationship under a given voltage:

$$Q = CV \quad \text{... Eq. (4.6)}$$

Where,

V : is the applied voltage, Q : charge applied, and C : the capacitance.

Sweeping the voltage with time gives:

$$C = \frac{\frac{dQ}{dt}}{\frac{dV}{dt}} = \frac{I}{S} \qquad \text{... Eq. (4.7)}$$

Hence, taking the current starting from 0 to either maximum anodic or cathodic current going in one direction either positive or negative direction. In this case cathodic current has maximum region above 0 current horizontal line and hence whole current is integrated in both positive and negative direction and an average of it is taken because if only the cathodic region current is considered then the resultant capacitance value will be very high in comparison to the actual value.

Cyclic voltammetry (CV) offers a rapid and proven method to discern whether bacteria use mobile redox shuttles to transfer their electrons, or pass the electrons "directly" through membrane associated compounds (*21*). For CV, a reference electrode is placed in the anode chamber of the MFC close to the anode (working electrode); the counter electrode (e.g., platinum wire) is preferably placed in the cathode chamber, but can also be placed in the anodechamber. A potentiostat is used to obtain a scan of potential. For bacterial suspensions, a scan rate of 25 mV s-1 appears to be reasonable based on the work of several researchers (*21*, *22*). For the analysis of mediators in biofilms, however, this scan rate needs to be decreased, possibly to 10 mV s-1 and lower. This decrease can affect the accuracy of peak discrimination as the peaks tend to broaden. The extent of the redox mediation and the midpoint potentials can be determined through analysis of (*i*) the MFC derived culture within its medium; (*ii*) the MFC culture after centrifugation and resuspension in physiological solution; and (*iii*) the supernatant of the centrifuged MFC culture. If a peak is found both in case (*i*) and (*ii*), it indicates a shuttle which is membrane associated. If a peak is found in case (*i*) and (*iii*), it indicates that a mobile, suspended shuttle is present. The size

of the peaks, as integrated upon the voltammogram, either arbitrarily (as ª[¢I¢E *ä*-1]) or through convolution analysis, does not correlate unequivocally to the extent of the membrane associated electron transfer and the mobile shuttle mediated electron transfer. This is caused by the restricted accessibility of the membrane associated shuttles for oxidation/reduction by the working electrode.[23,21,25]

Presence of Nanowires. Electrically conductive bacterial appendages known as nanowires have only recently been discovered so their structure(s) are therefore not well studied or understood. Pili produced by some bacteria have so far been shown to be electrically conductive using scanning tunneling electron microscopy (*26*). There is no data at the present time whether nanowires can be detected or can be distinguished from adsorbed chemical shuttles via standard electrochemical methods such as CV. If electron shuttles associate with a nonconductive pili, or if the pili are covered with metal precipitates, they will be included in the CV measurements as membrane associated shuttles or may appear to be nanowires using STM. If redox shuttles are enclosed within the pilus' tubular structure they are unlikely to be detected using CV. Additional research will be needed to determine the best methods for detecting nanowires and determining their importance relative to other methods of electron transfer from cells to electrodes.

The electrochemical Impedance spectroscopic technique is used to study the changes occurring at the interface of the electrode and solution as it is sensitive and is capable of providing information about the modification carried out on an electrode surface. It is a powerful technique that reveals the changes occurring in the charge transfer processes at the electrode/solution interface. The resistance is given by Ohm's law: R = E/I, when a DC signal is applied to an interface where, E and I are the applied voltage and resulting current, respectively. When an AC signal is applied to an interface, Ohm's law is again applicable, but the measured quantity is called

the impedance Z = Ep/Ip, where Ep and Ip are the applied peak voltage and the measured peak current respectively. The AC impedance technique is commonly applied to the investigations of electrode kinetics and the reaction rates are related to the charge transfer resistances. Electrochemical Impedance is usually measured by applying an AC potential to an electrochemical cell and measuring the current through a cell.[27,28]

EIS measurements were carried for the MFC in the frequency range from 4400 Hz to 3 Hz with an AC signal of 50 mV amplitude. For EIS measurements of whole MFC cathode was used as the reference and counter electrode and the anode was used as the working electrode [29].

Figure 4.8 Electrochemical Analyzer (Metrohm Autolab AUT-85279)

4.4.5 Four Probe Conductivity Measurement

At a constant temperature, the resistance, R of a conducting substance is directly proportional to its length L and inversely proportional to its cross-sectional area A.

$$\boldsymbol{R = \frac{\rho L}{A}} \qquad \ldots \mathbf{Eq.(4.8)}$$

Where ρ is the resistivity of the conducting substance and its unit is ohmmeter.

A semiconductor has an electrical conductivity in between the magnitude of a conductor and an insulator. Semiconductors differ from metals in their characteristic property of decreasing electrical resistivity with increasing temperature.

According to band theory, the energy levels of semiconductors can be grouped into two bands, valence band, and the conduction band. In the presence of an external electric field, it is electrons in the valence band that can move freely, thereby responsible for the electrical conductivity of semiconductors. In the case of intrinsic semiconductors, the Fermi level lies in between the conduction band minimum and valence band maximum. Since conduction band lies above the Fermi level at 0K, when no thermal excitations are available, the conduction band remains unoccupied. So conduction is not possible at 0K, and resistance is infinite. As temperature increases, the occupancy of conduction band goes up, thereby resulting in a decrease of electrical resistivity of the semiconductor.

The resistivity of the semiconductor can be calculated by four probe method as follows:

1. The resistivity of material is uniform in the area of measurement.

2. If there is a minority carrier injection into the semiconductor by the current- carrying electrodes most of the carriers recombine near electrodes so that their effect on conductivity is negligible.

3. The surface on which the probes rest is flat with no surface leakage.

4. The four probes used for resistivity measurement contact surface at points that lie in a straight line.

5. The diameter of the contact between metallic probes and the semiconductor should be small compared to the distance between the probes.

6. The boundary between the current carrying electrodes and the bulk material is hemispherical and small in diameter.

7. The surface of semiconductor material may be either conducting and non-conducting. A conducting boundary is one on which material of much lower resistivity than semiconductor has been plated. A non-conducting boundary is produced when the surface of the semiconductor is in

contact with an insulator.

The figure shows the resistivity probes on a die of material. If the side boundaries are adequately far from the probes, the die may be considered to be identical to a slice. For this case of a slice of thickness w and the resistivity is computed as

$$\rho = \frac{\rho_o}{f(\frac{w}{s})}$$

... Eq. (4.9)

The function, f(w/S) is a divisor for computing resistivity which depends on the value of w and S

We assume that the size of the metal tip is infinitesimal and sample thickness is greater than the distance between the probes,

$$\rho_o = \frac{V}{I} 2\pi S$$

... Eq. (4.10)

Where,

V – the potential difference between inward probes in volts.

I – Current through the outer pair of probes in ampere.

S – Spacing between the probes in the meter.

Effect of temperature in the resistivity of semiconductor

The total electrical conductivity of a semiconductor is the sum of the conductivities of the

conduction band and valence band carriers. Resistivity is the reciprocal of conductivity and its temperature dependence is given by

$$\rho = A\, exp \frac{E_g}{2KT}$$

... Eq. (4.11)

Where,

K – Boltzmann constant, K = 8.6x10-5 eV/K

Eg – band gap of the material

T – Temperature in Kelvin

On decreasing the temperature the resistivity of a semiconductor rises exponentially.

The experimental setup consists of an oven (0-200°C), probes arrangement, constant current source, sample, digital panel meter (for voltage and current measurement) and an oven power supply.

Four probe setup is one of the ideal and most widely used setups for measuring the resistivity of semiconductors. In order to employ this method, the sample should be in the form of a thin wafer. The sample is in dimensions of millimeters in size and having a thickness w. Four probes are arranged linearly in a straight line at equal distance S from each other. A constant current flows through the two probes and the potential drop V across the middle two probes is measured. An oven is provided with a heater to heat the sample so that behaviour of the sample is studied with an increase in temperature.

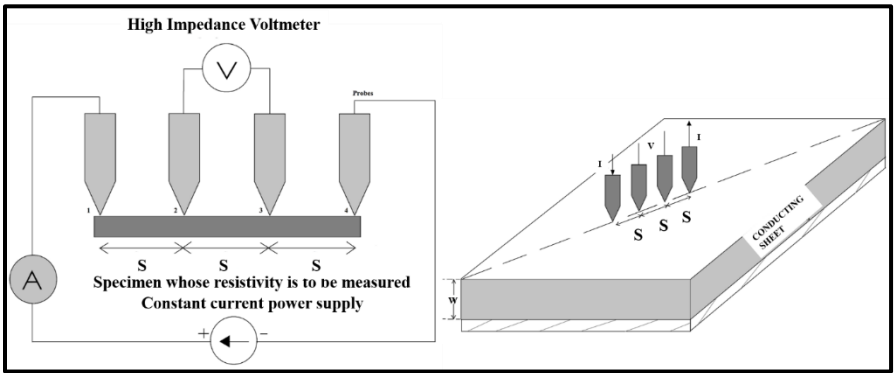

Figure 4.9 Four probe conductivity measurement

Figure 4.10 Four probe conductivity measurement

4.4.6 Measurement of thickness of electrode using digital micrometer

Figure 4.11 Digital micrometer (Mitutoyo MDC 25SX)

A micrometer (or micrometer screw gauge) is a device including a calibrated screw widely used for accurate measurement of the thickness of components like sheets etc. Micrometers are usually in the form of calipers (opposing ends joined by a frame). The spindle is a very precisely machined screw and the object to be measured is placed between the anvil and the spindle. The spindle is moved by turning the ratchet knob or thimble until the object to be measured is lightly touched by both the spindle and the anvil.

The model which we used was Mitutoyo MDC 25SX. It is a digital micrometer and we measured the thickness of the graphite paste coated aluminium electrodes and other modified electrodes prepared in order to calculate their resistivity by four probe method with the help of it.

4.4.7 Measurement of current and potential from MFC using Keithley 2000 Digital Multimeter

Figure 4.12 Keithley 2000 Digital Multimeter for current and potential measurement

In order to measure two or more electrical values—principally voltage (volts), current (amps) and resistance (ohms) test tool like a digital multimeter is used. It is mostly used by scientists and technicians in the electrical/electronic industries.

Needle-based analog meters were replaced by digital multimeters due to their capacity to measure with greater precision, reliability and increased impedance.

Digital multimeters combine the testing capabilities of single-task meters—the voltmeter (for measuring volts), ammeter (amps) and ohmmeter (ohms). Often they include a number of additional specialized features or advanced options. Technicians with specific needs, therefore, can seek out a model targeted for particular tasks.

The face of a digital multimeter includes four parts:

- Display: Where measurement readouts can be viewed.
- Buttons: For selecting various functions; the options vary by model.
- Switches: For selecting primary measurement values (volts, amps, ohms).

- Input jacks: Where test leads are inserted.
- RS-232 cable port for connecting with PC
- GPIB cable port for connecting with PC.

Test leads are bendable, insulated wires (red insulation for positive and black insulation for negative) that plug into the DMM. They serve as a connection from the item being tested to the multimeter. Circuits are tested using probe tips. Terms like counts and digits are used to refer to a digital multimeter's resolution (how fine a measurement a meter can make). By knowing a multimeter's resolution, a technician can determine if it is possible to see a small change in a measured signal. Digital multimeters are typically grouped by their number of counts (up to 20,000) they display.

Measurement of open circuit voltage (OCV)

EMF of a cell is a thermodynamic value and it does not take internal losses into account. Open Circuit voltage is the difference of electrical potential between the two terminals of a device at infinite load. OCV theoretically should reach the cell EMF but practically it is somewhat lower than the EMF of the MFC due to various potential losses.

We measured the open circuit voltage between the anode and the cathode with the help of digital multimeter (Keithley 2000) for 52 days at an interval of 10 minutes. This experiment was done only for bigger MFC in order to know the behaviour of open circuit voltage of MFC during day and night.

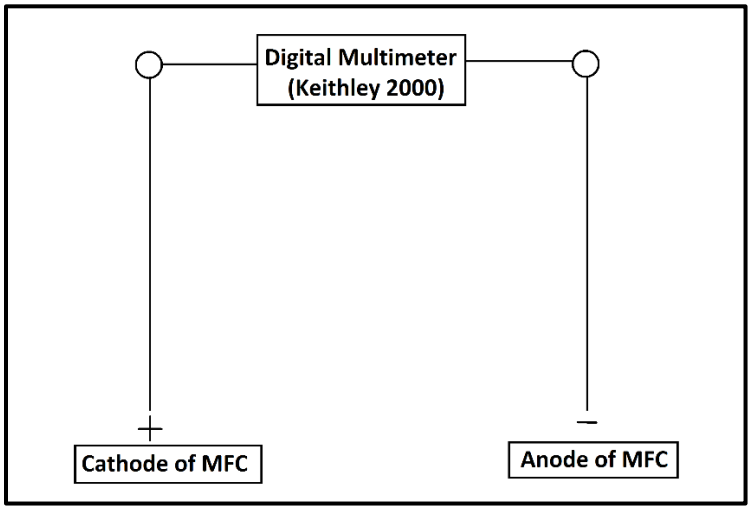

Figure 4.13 Equivalent circuit for measuring the open circuit voltage of microbial fuel cell

Measurement of Potential across 51.0977, 145.776, 982, 9767.3, 15003,5, 99245.7 Ω resistances

We measured the potential between the anode and the cathode with the help of digital multimeter (Keithley 2000). External resistances of 51.0977, 145.776, 982, 9767.3, 15003,5, 99245.7 Ω were connected one by one between the electrodes of the MFC and the potential drop gainst them was measured. Figure 4.14 shows the Schematic of the load resistance connected to the MFC.

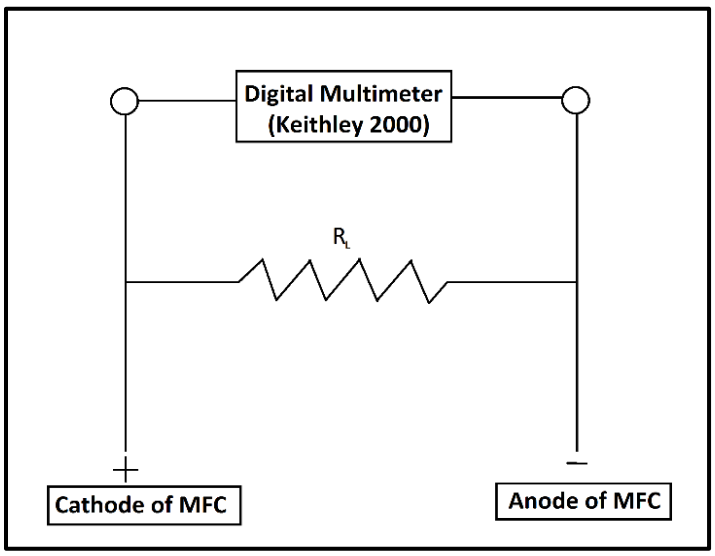

Figure 4.14 Equivalent circuit of load resistance connected to MFC

Measurement of current across 9767.3 Ω resistance

Current flowing through the load resistance was measured as shown in the schematic in figure 4.15 with the help of digital multimeter (Keithley 2000).

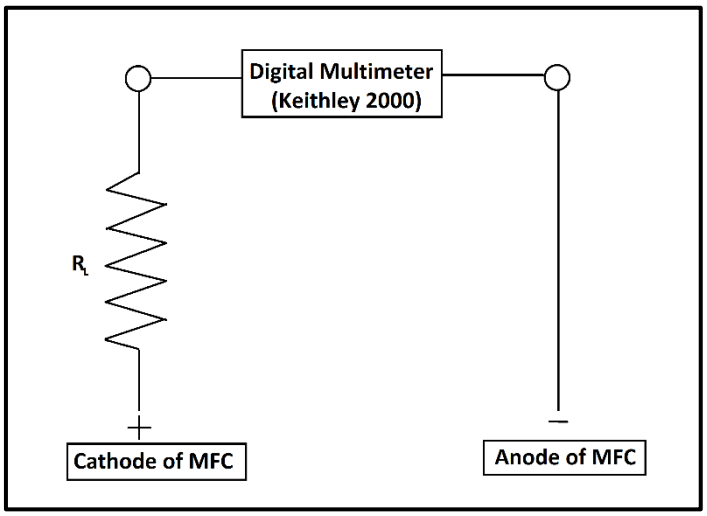

Figure 4.15 Current measurement through 9767.3 ohm resistance

4.4.7 Energy Losses

Measured cell voltage in an MFC is a linear function of current measured. It is used to calculate the energy loss.

Energy losses in an MFC can be calculated using the formula:

$$V_{device} = OCV - IR_{internal} \quad \text{...Eq. (4.12)}$$

Where V_{device} represents the actual voltage of the device and is equal to the difference between Open Circuit Voltage (OCV) and peak current times internal resistance of the device. $IR_{internal}$ represents the energy loss. $IR_{internal}$ is the sum of all internal losses of the MFC, which are proportional to the generated current (I) and internal resistance of the system (R_{int}).

Energy loss calculation in the graphite paste/Al anode based system could be used to obtain a better understanding of how to get the maximum energy output under these conditions, as well as the possible causes of energy loss in these systems.

4.4.8 Thermodynamics involved in MFCs

When a reaction is thermodynamically favourable i.e. Gibbs free energy is negative, then only electricity could be produced from an MFC.

$$\Delta G_r = \Delta G_r^\circ + RT ln(Q) \quad \text{...Eq. (4.13)}$$

Where, Q is the reaction quotient and has no unit, ΔG_r is Gibbs free energy at specific condition and has unit Joule(J), ΔG_r° is the Gibbs free energy at standard state condition and has unit Joule(J), R is the ideal gas constant and has value equal to 8.314 J/mol-K, and T is the temperature in Kelvin(K).

In the case of MFCs calculation of cell EMF (E_{emf}(V)) (which is the potential difference between anode and cathode) can be related to work(J) produced by the cell.

i.e.

$$W = E_{emf} q = -\Delta G_r \quad \text{... Eq. (4.14)}$$

$$q = nF \quad \text{... Eq. (4.15)}$$

Where q is the charge transferred in the reaction in Coulombs, n is the number of electrons exchanged in the reaction and F is the Faraday's constant.

$$E_{emf} nF = -\Delta G_r \quad \text{... Eq. (4.16)}$$

$$E_{emf} = -\frac{\Delta G_r}{nF} \quad \text{... Eq. (4.17)}$$

$$\Delta G_r = -nFE_{emf} \quad \text{... Eq. (4.18)}$$

At standard conditions,

Reaction Quotient (Q) = 1

$$E^\circ_{emf} = -\frac{\Delta G_r^\circ}{nF} \quad \text{... Eq. (4.19)}$$

$$\Delta G_r^\circ = -nFE_{emf}^\circ \quad \text{... Eq. (4.20)}$$

$$\Delta G_r = \Delta G_r^\circ + RTlnQ \quad \text{... Eq. (4.21)}$$

$$-nFE_{emf} = -nFE_{emf}^\circ + RTlnQ \quad \text{... Eq. (4.22)}$$

$$E_{emf} = E_{emf}^\circ - \frac{RT}{nF}lnQ \quad \text{... Eq. (4.23)}$$

Where, E_{emf} is the electromotive force and E_{emf}° is the standard electromotive force. Hence, the above equation expresses the overall reaction in terms of the potentials. Above equation produces a positive value of E_{emf} for favourable reactions and gives an upper limit for voltage MFC voltage for that particular reaction. Due to various potential losses, the actual value of MFC potential would be lower than E_{emf}.

Half cell reactions i.e. separate reactions occurring at cathode and anode can be used to analyse MFC reactions.

$$E_{emf} = E_{cathode} - E_{anode} \quad \text{... Eq. (4.24)}$$

For eg- if bacteria at anode oxidize glucose we write reaction as:

$$6CO_2 + 24e^- \rightarrow C_6H_{12}O_6 \qquad Potential = -0.50V$$

Standard potentials are expressed relative to Normal Hydrogen Electrode (having 0 potential at standard condition).

Theoretical anode potential can be calculated by using the equation:

$$E_{emf} = E^\circ_{emf} - \frac{RTlnQ}{nF} \qquad \text{... Eq. (4.25)}$$

$$E_{anode} = E^\circ_{anode} - \frac{RT}{24F}\ln\left(\frac{[C_6H_{12}O_6]}{[CO_2]^6}\right) = -0.50 - 0.00106993\ln(\frac{[C_6H_{12}O_6]}{[CO_2]^6})$$

The cathodic reaction can be written as:

$$[Fe(CN)_6]^{3-} + e^- \rightarrow [Fe(CN_6)]^{4-} \qquad Potential = 0.361V$$

Theoretical cathode potential can also be calculated using the equation:

$$E_{cathode} = E^\circ_{cathode} - \frac{RT}{F}\ln\left(\frac{[Fe(CN)_6]^{4-}}{[Fe(CN)_6]^{3-}}\right) = 0.361\,V$$

Hence, overall MFC emf can be calculated as:

$$E_{emf} = E_{cathode} - E_{anode}$$

$$= 0.361 - \left(-.50 - .304760.00106993\ln\left(\frac{[C_6H_{12}O_6]}{[CO_2]^6}\right)\right)$$

$$= .861 + .304760.00106993\ln\left(\frac{[C_6H_{12}O_6]}{[CO_2]^6}\right)$$

When $[C_6H_{12}O_6] = 0$, then E_{emf} will be undefined

When $[CO_2] = 0$, then E_{emf} will be infinity

When $[C_6H_{12}O_6] = [CO_2]$, then E_{emf} will be equal to 0.861 V

When $[C_6H_{12}O_6] > [CO_2]$, then E_{emf} will be > 0.861 V.

CHAPTER-5

5. RESULTS AND DISCUSSION

5.1. Morphological analysis using Scanning Electron Microscopy

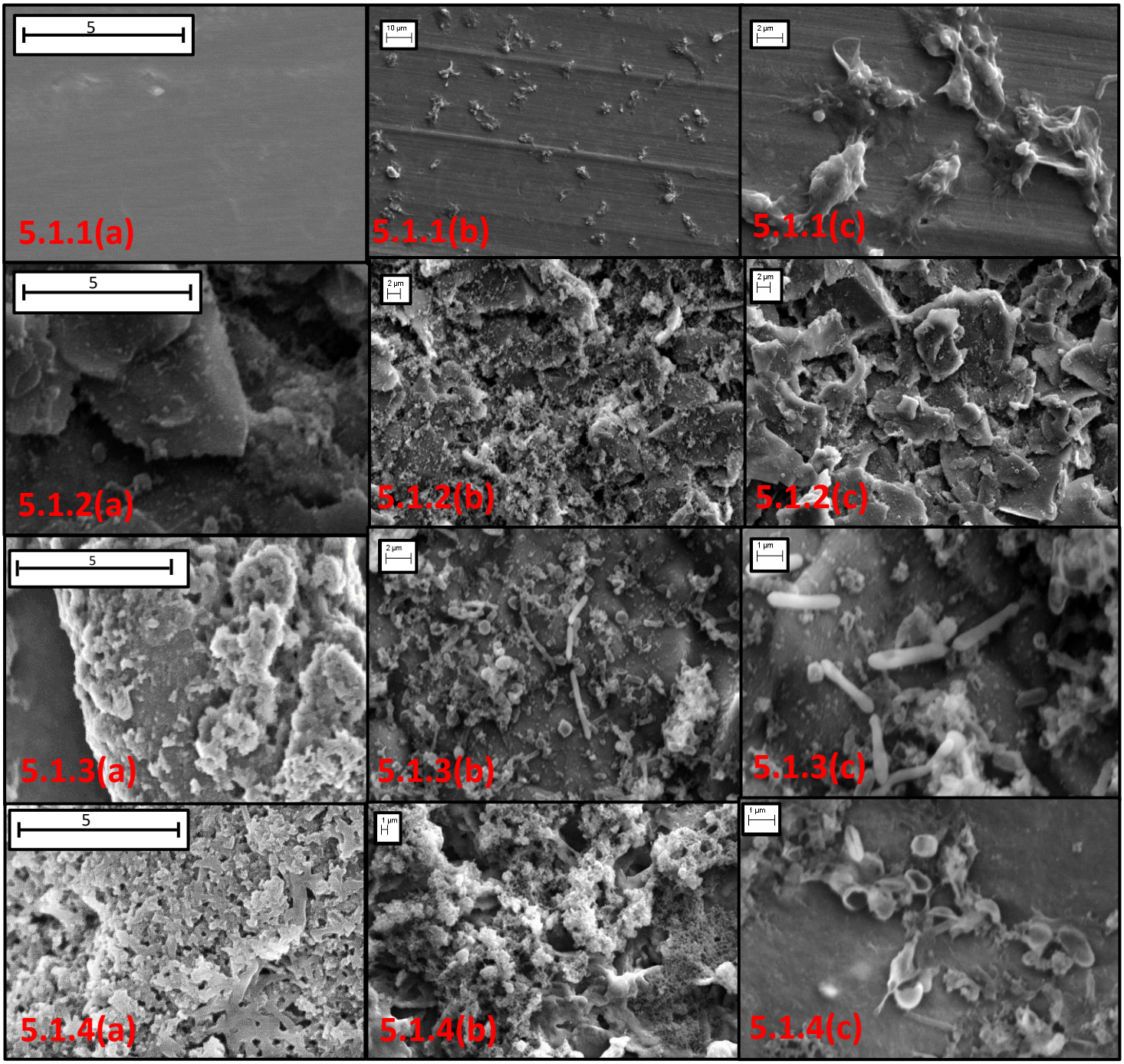

Figure 5.1 Surface morphology of aluminium (5.1.1(a-c)), Graphite paste/Al (5.1.2(a-c)), rGO/Graphite paste/Al (5.1.3(a-c)) and PANI/rGO/Graphite paste/Al (5.1.4 (a-c)). Substrates 5.1.1(b,c)-5.1.4(b,c) are with microbes and 5.1.1(a)-5.1.4(a) are without microbes.

Rotten potato paste diluted with equal volume of DI water and then different electrode materials were dip inside the solution for 7-days at an incubation temperature of 37°C. Figure 5.1.1(a), 5.1.2(a), 5.1.3(a) and 5.1.4(a) show surface morphology of different electrode materials: Al, Graphite paste/Al, rGO/Graphite paste/Al and PANI/rGO/Graphite paste/Al respectively. Aluminium foil appeared as a flat plain surface. Graphite paste depicted flake like structure as reported elsewhere while SEM images of rGO/Graphite paste/Al indicating granulated form of rGO on graphite flakes. Further, interconnected network like structure of PANI in Figure (5.1.4(a)) indicating typical structure of PANI as appeared after polymerization.

Microbes cultured on aluminium surface were find to have distorted morphology as shown in Figure No. 5.1.1(b) and 5.1.1(c). It indicates aluminium material could not be used as an electrode material. Surprisingly, no microbes were visible on the surface of graphite flakes 5.1.2(b) and 5.1.2(c), it could deduced that microbes might be present beneath the flakes of graphite, thus could not be visualized on the surface. Some microbes having fully distorted shapes were visible on the PANI surface this might indicating toxicity of the polymer. Thus, PANI might showing the characteristics of the antimicrobial substrate. Microbes having characteristic rod like structure appeared on the surface of rGO/graphite paste/Al (Figure 5.1.3(b) and 5.1.3(c)). rGO enhance the surface compatibility and surface area which might favoured the microbial growth.

Thus, only rGO/Graphite paste/Al found to be a more suitable substrate for microbial culture as relative to Al, PANI, graphite surfaces.

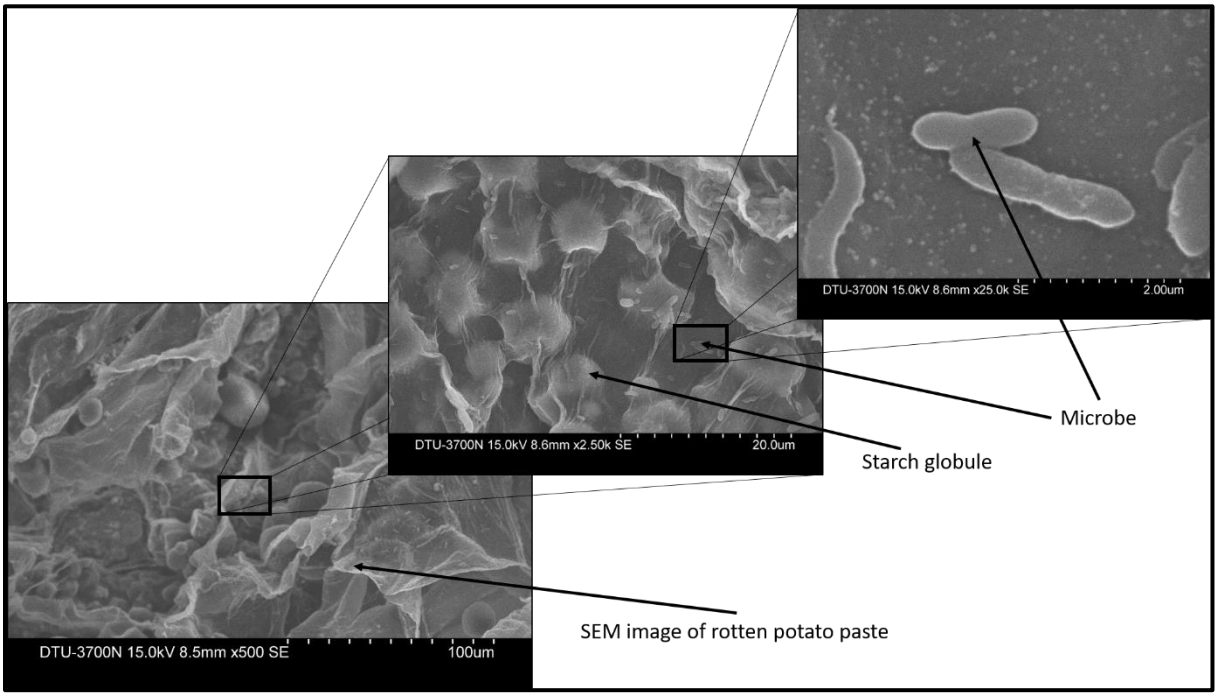

Figure 5.2 Scanning electron microscopy of rotten potato paste and microbes.

Starch globules are present in the sac like structure as shown in SEM images (Figure 5.2). At higher magnification (25,000X) bacilli could be observed. This potato waste was further used as a microbial source in MFCs where fermenting microbes can directly utilize starch and glucose present in potato slurry.

5.2. Four points probe conductivity measurement of electrodes used

Graphite paste/Al gave a conductivity of 0.4355 S/m. rGO/Graphite paste/Al gave a conductivity of 0.52 S/m whereas PANI/rGO/Graphite paste/Al gave a conductivity value of 0.56 S/m. Thus, incorporation of rGO enhanced the conductivity upto 19.40 % to that of Graphite paste/Al while slight increase in conductivity of 7.69 % was observed in PANI/rGO/Graphite paste/Al in relative to rGO/Graphite paste/Al electrode. Thus, increase in conductivity along with increased surface area in case of PANI/rGO/Graphite paste/Al and rGO/Graphite paste would

probably enhance electron transfer from microbes to the electrode leading towards increased current density in MFCs.

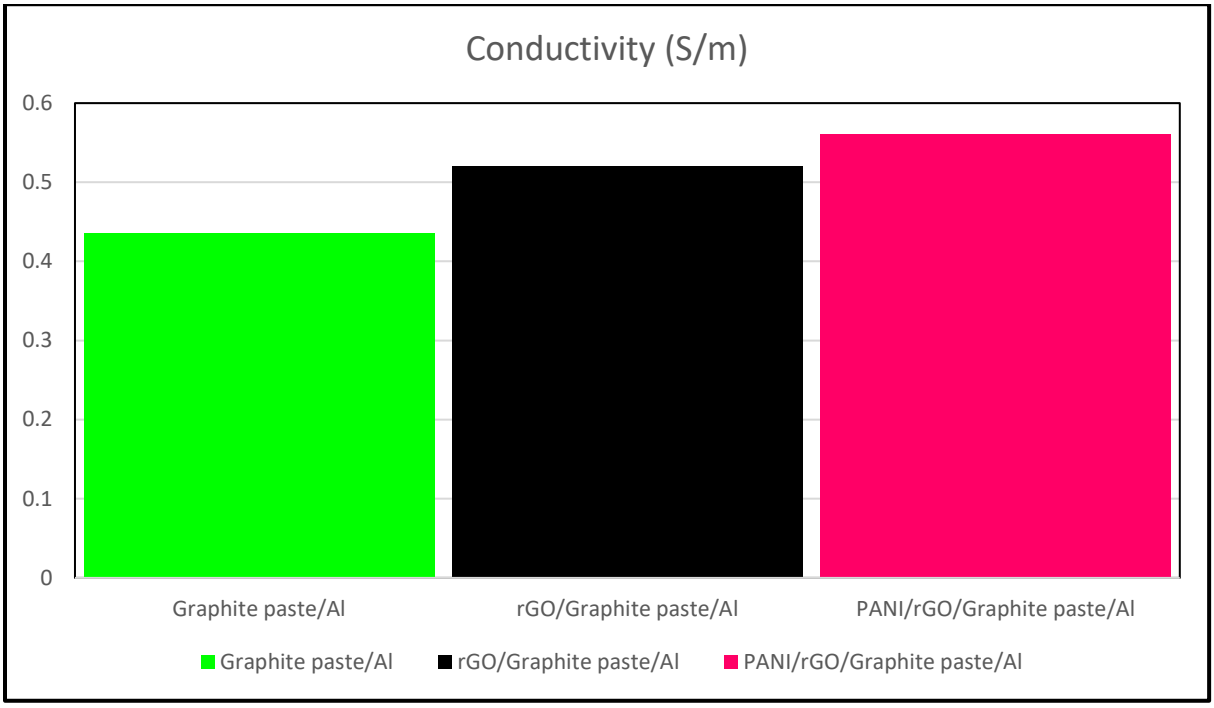

Figure 5.3 Electrical Conductivity (S/m) of different electrode materials for MFCs

5.3. Cyclic Voltammetry studies

Cyclic voltammogram of all the electrodes appeared to be irreversible.[30] The area of CV curve which denotes specific capacitance values for different electrode materials was in the order Al > PANI/rGO/Graphite paste/Al > Graphite paste/Al > PANI/Graphite paste/Al > rGO/Graphite paste/Al. This further confirmed to use rGO/Graphite paste/Al as our electrode material as it showed the least capacitive behaviour in comparison to other materials used. Hence, from this study we found out that rGO/Graphite paste/Al and Graphite paste/Al electrodes are better materials in comparison to Al, PANI/rGO/Graphite paste/Al it they undergo low oxidation and reduction in comparison to the latter used.

Moreover, coating of graphite paste found to prevent the Al corrosion during this electrochemical study.

High conductivity indicate fast electron transfer rate which could further enhance the efficiency of MFCs.

Al when used along will get corroded very easily in comparison to its coated counterparts.

Sr. No.	**Material of Electrode**	**Area of Cyclic Voltammogram**	**Average current(I)**	**[C=(I/s)] in Farad**
1.	Al	.002998	.001499	.02998
2.	Graphite paste/Al	.002244	.001122	.02244
3.	PANI/Graphite paste/Al	.001816	.000908	.01816
4.	rGO/Graphite paste/Al	.001459	.0007295	.01459
5.	PANI/rGO/Graphite paste/Al	.002673	.0013365	.02673

Table 5.1 Calculation of Capacitance of different electrode materials from cyclic voltammetry data

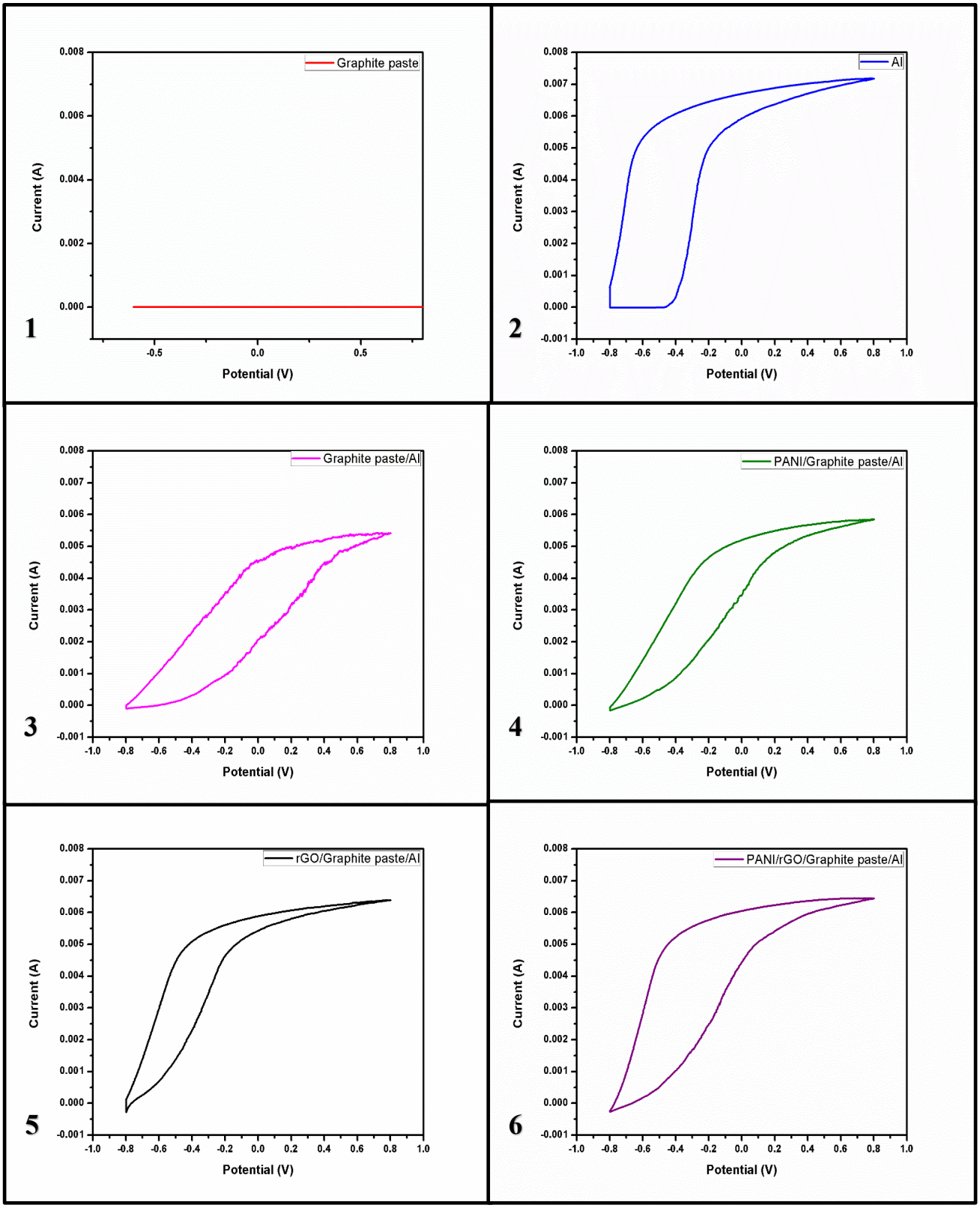

Figure 5.4 Cyclic Voltammetry of different electrode materials (1) Graphite paste, (2) Al, (3) Graphite paste/Al, (4) PANI/Graphite paste/Al, (5) rGO/Graphite paste/Al, (6) PANI/rGO/Graphite paste/Al

5.4. Open Circuit Voltage Measurement

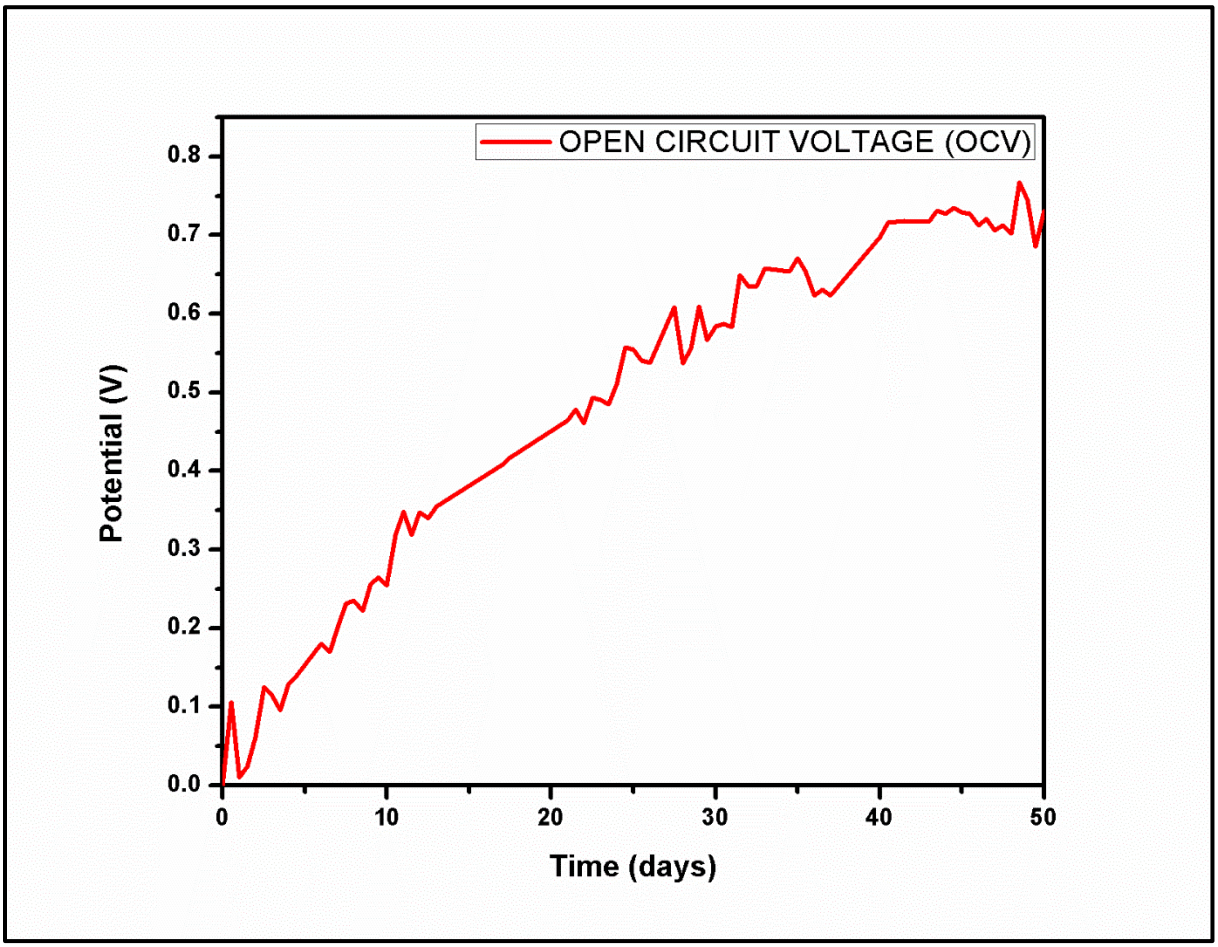

Figure 5.5 Open Circuit Voltage (OCV) graph for H shaped Microbial Fuel Cell (MFC).

H-shaped MFC gave the peak OCV of 750 mV and miniaturized MFC gave a peak OCV of 671.2 mV. OCV of H shaped MFC consistently increased for 42 days until saturation attained. Fluctuations in the graph indicating variation in temperature, light and humidity in the surrounding of fuel cell. High temperature at

day time enhances metabolic activity of microbes and hence the OCV increases while low temperature at night decrease microbial metabolic activity as a result the OCV value also decreases.

OCV values in an MFC can be used to calculate the energy losses using the formula:

$$V_{device} = OCV - IR_{internal} \quad \text{... Eq. (5.1)}$$

5.5. Voltage vs time across different load resistances

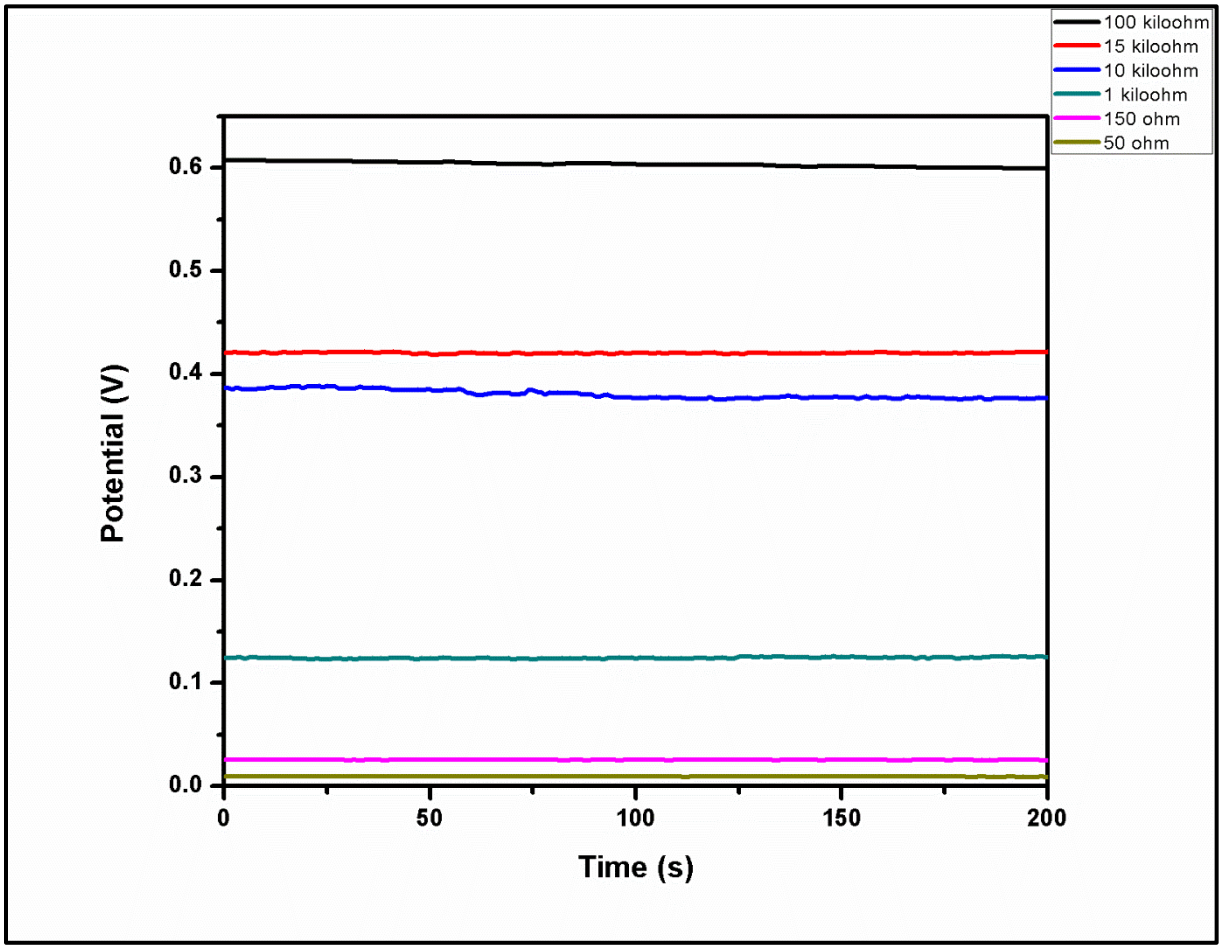

Figure 5.6 Potential vs time curve for H shaped MFC across different load resistances

Sr. No.	Resistance	Potential (V)
1	50 Ω	0.00894
2	150 Ω	0.0254
3	1 kΩ	0.12528
4	10 kΩ	0.37555
5	15 kΩ	0.42105
6	100 kΩ	0.59823

Table 5.2 Potentials across different resistances for H-shaped MFC

In Open Circuit i.e. at infinite load, maximum voltage is obtained from an MFC. On decreasing the load resistance (R_{load}) the voltage of MFC also decreases. However, the theoretical energy gain for microbes is controlled by the anode potential. At low anode potential, the redox potential at the anode was probably too low to make it a favorable electron acceptor for the microorganisms, i.e., there is low energy per electron transferred available for cell maintenance and growth. Thus, the differences in MFC output with different external resistances may be associated with variations in activation losses at the anode, which is a function of electrochemical activity of anode-reducing microorganisms. Therefore, there exists an optimum anode potential enabling the microbes to balance electrode reduction kinetics with potential energy gain, which could be easily achieved through selection of the appropriate external resistance. The activation losses have less impudence on the MFC operation at a suitable external resistance, which occurs when external resistance is close to the internal one. [31]

As shown in figure 5.7, the plot is linear upside as well as downside but, in the middle region there is a slight peak showing optimum resistance for H-shaped MFC at a resistance of 10 kΩ.

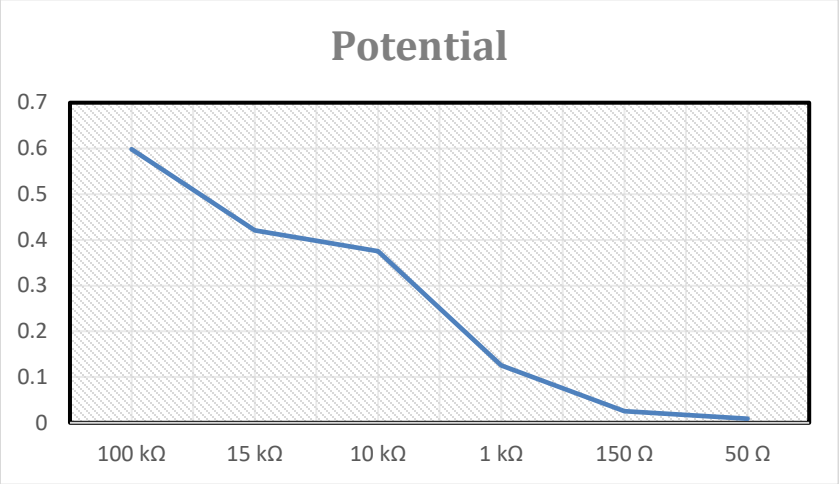

Figure 5.7 Potential of H-shaped MFC across different resistances

5.6. Current vs time for different load resistances

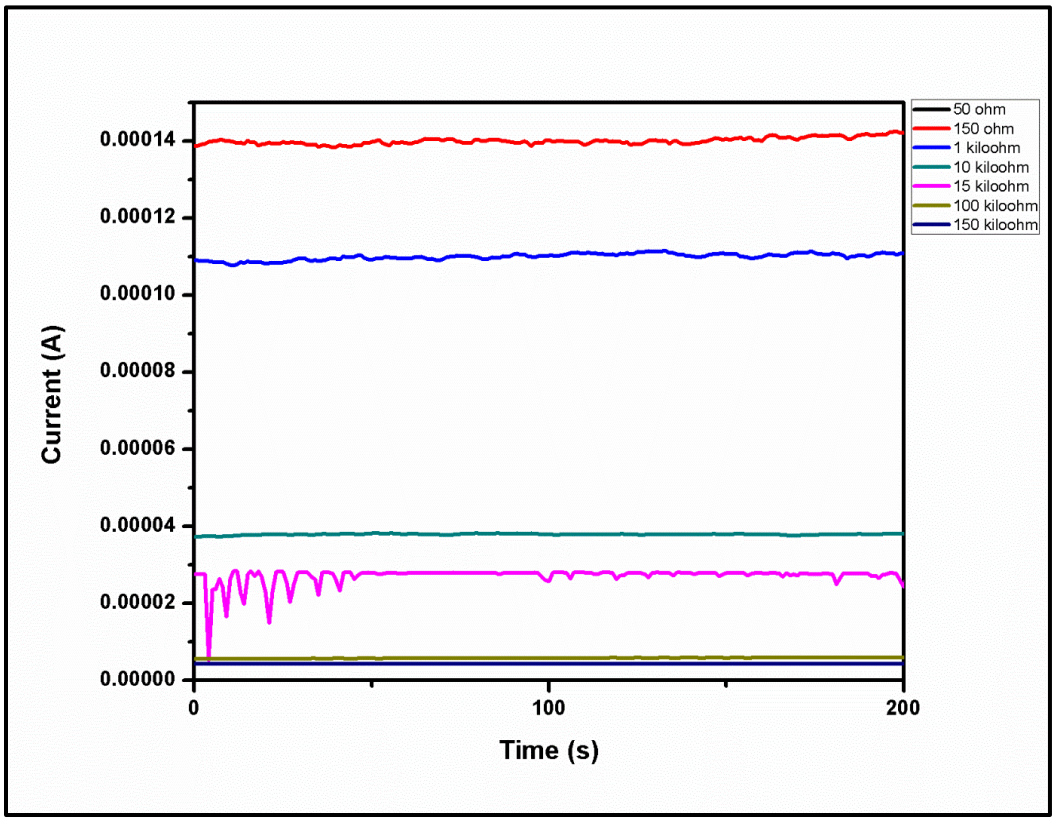

Figure 5.8 Current vs time curve for different resistances in H-shaped MFC

Sr. No.	Resistance	Current (A)
1	150 Ω	1.43823E-4
2	1 kΩ	1.11688E-4
3	10 kΩ	3.78E-5
4	15 kΩ	2.82E-5
5	100 kΩ	6.13E-6
6	150 kΩ	4.38E-6

Table 5.3 Current flowing through different resistances for H-shaped MFC

When MFC is operated with a low load resistance, the MFC generates higher current because of the highest electron transfer to the cathode supporting high electrogenic activity and rapid cathode reaction. Similarly, various studies have observed improved current generation over time with stepwise decreases in the external resistance of an MFC. In the study of Aelterman et al., the descent of external resistance from 50 to 25Ω and finally to 10.5Ω resulted in a significant increase in the continuous current generation. Similarly, in our study also the descent of external resistance from150kΩ to 50Ω also resulted in a significant increase in the continuous current generation. Moreover, Aeltermant et al. observed that when the MFCs were operated at lower resistances, the mass transfer or kinetic limitations observed during polarization lowered, resulting in a less steep descent of the current density.[31]

Effects of Load Resistance on Microbial Fuel Cell's Performance

For MFCs working at low load resistance, a minor increase in internal resistance can sturdily decrease the MFCs performance which reduces the current production mainly because of the internal resistance but not due to the external load.

For MFCs working at high load resistance limits the current that is able to flow from anode to cathode, and this may affect which microorganisms are able to colonize the anode. Furthermore, in this case, the limiting element is the load resistance, and the current production is almost

independent of another factor, such as the distance between the electrodes and the anode surface.[31]

5.7. Power Density vs time across different load resistances

When the load resistance R_{load} is high, then the cell voltage is high and current is low and vice versa. Since, power is the product of cell voltage and current. Therefore, the optimisation of load resistance is a must in order to achieve the maximum power density.

If the load resistance R_{load} is low, then the equilibrium potential of the cell initially generates a high instantaneous electric current, higher than the maximum sustainable rate of charge transfer to/from the current-limiting electrode. As a result, the potential across the cell decreases quickly and adjusts to the rate of charge transfer to the current-limiting electrode, effectively decreasing the current in the external circuit. However, if the external circuit has a relatively high electrical resistance, then the equilibrium potential of the cell generates an electric current lower than the maximum sustainable rate of charge transfer to/from the current-limiting electrode. The potential of the cell adjusts to the load resistance. In the latter case, the power generation is sustainable but lower than it could be if the resistance of the external circuit were lower.

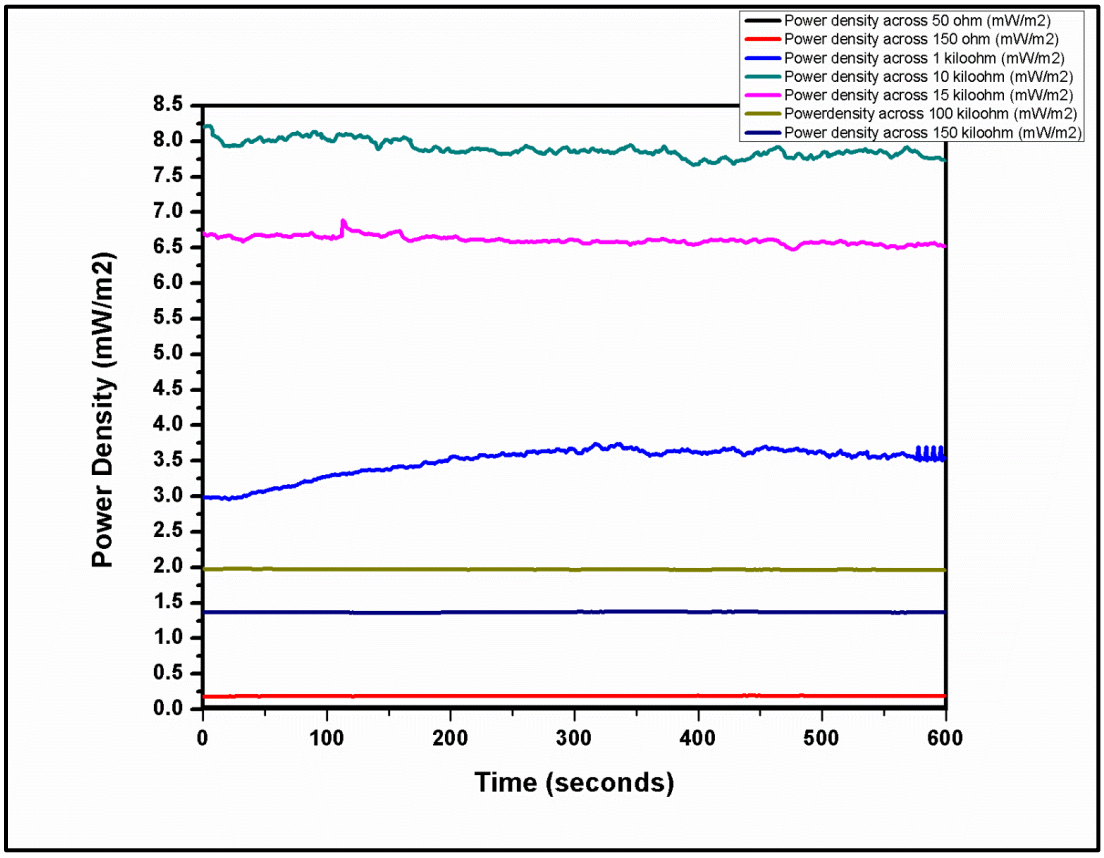

Figure 5.9 Power density vs time curve for H-shaped MFC across different load resistances

Power densities (mW/m^2) across different resistances were calculated to select an appropriate load resistance.

Sr. No.	Resistance	Power Density (mW/m^2)
1	50 Ω	0.0295
2	150 Ω	0.18121
3	1 kΩ	2.99429
4	10 kΩ	8.20352
5	15 kΩ	6.71111
6	100 kΩ	1.97513
7	150 kΩ	1.36559

Table 5.4 Power densities across different resistances for H-shaped MFC

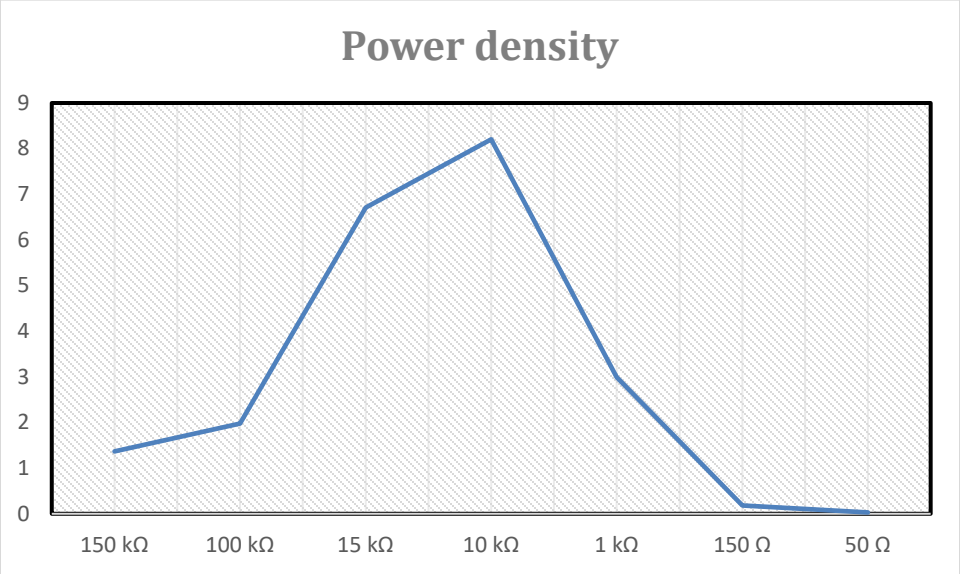

Figure 5.10 Power density vs resistance curve H-shaped MFC

It was found that MFC when connected across 10 kiloohm gives highest power density.

This could be explained on the basis of maximum power theorm, according to which maximum power is drawn when the load resistance or external resistance of power source (MFC) equals to the internal resistance of power source (MFC).

$$\boldsymbol{I = \frac{V}{R_{load} + R_{int}}}$$

... Eq. (5.2)

And the Power can be calculated as:

$$\boldsymbol{P = I^2 R_{load}}$$ ... Eq. (5.3)

$$\boldsymbol{P = \left[\frac{V}{R_{load}+R_{int}}\right]^2 R_{load}}$$ ... Eq. (5.4)

$$P = \left[\frac{V^2}{R_{load}^2 + R_{int}^2 + 2R_{load}R_{int}}\right] R_{load} \quad \text{... Eq. (5.5)}$$

On applying the principle of maxima and minima, we get maximum power only when, the denominator on the R.H.S is minimum i.e. on maxima and minima the first derivative is equal to 0.

$$\frac{d\,[R_{load}^2 + R_{int}^2 + 2R_{load}R_{int}]}{dR_{load}} = 0$$

$$-\frac{R_{int}^2}{R_{load}^2} + 1 = 0$$

$$\frac{R_{int}^2}{R_{load}^2} = 1$$

Therefore, theoretically there is maximum power only when,

$$R_{int} = R_{load}$$

Since, this power density reading was taken during the starting days of H shaped MFC, therefore, it concludes that at the starting point the internal resistance of H shaped MFC was near 10 kiloohm.

5.8. Internal Resistance vs time

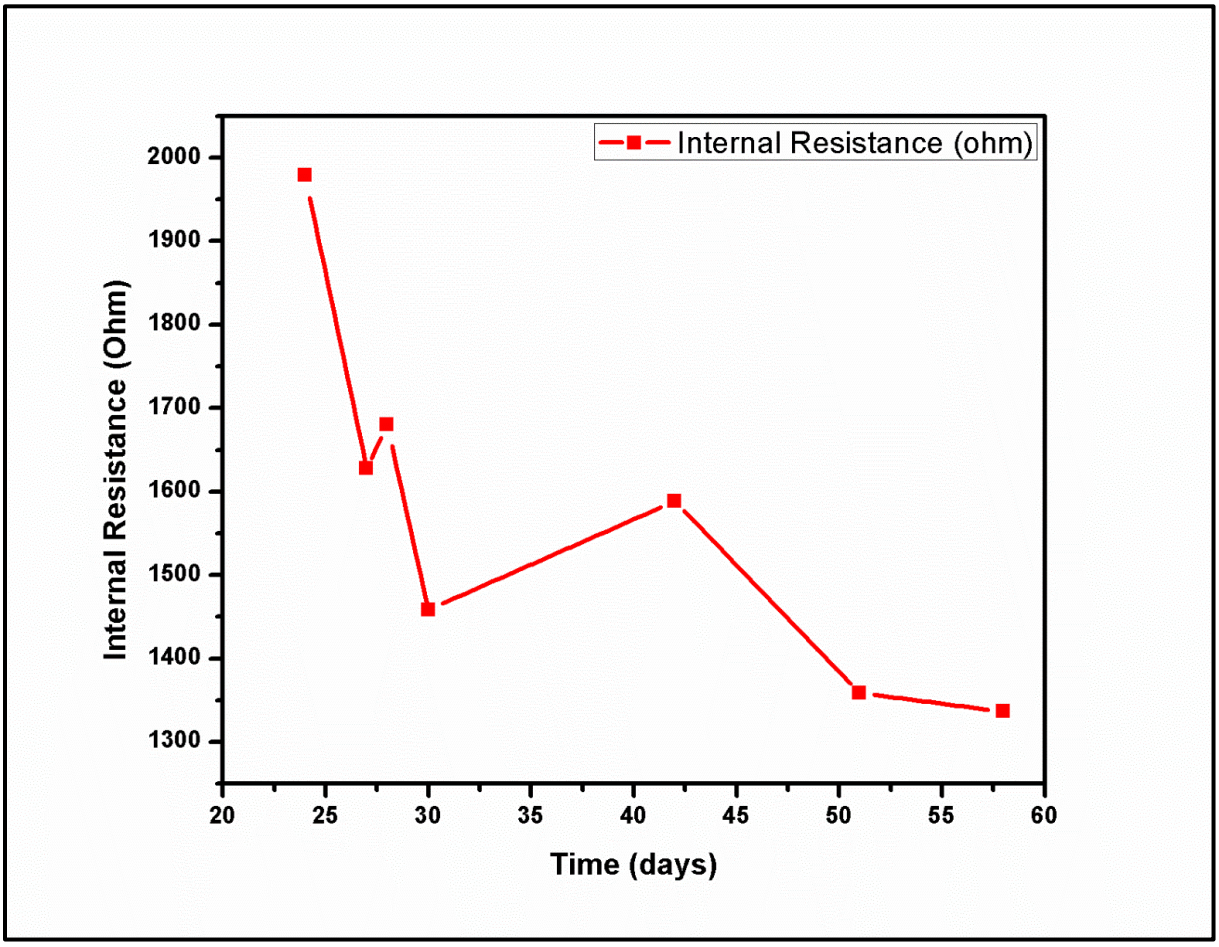

Figure 5.11 Internal Resistance measurement for H shaped MFC for 60 days using Electrochemical Impedance Spectroscopy

Measurements in H shaped MFC were done for a period of 60 days and EIS measurements were made in between at regular intervals. Internal Resistance (R_{in}) for MFC decreased from approximately 1979.49 Ω on 24th day to about 1336.31 Ω on 58th day.

Table 5.5 Internal Resistance measurements of H-shaped MFC

Sr. No.	Day	Internal Resistance
1	24	1979.49
2	27	1627.6
3	28	1680.07
4	30	1458.5
5	42	1588.77
6	51	1358.53

7	58	1336.31

Hence, for MFCs working for longer periods of time, the internal resistance decreases from a higher value to a lower value might be due to increase in the growth of microbes over anode surface leading to decrease in the value of charge transfer resistance (R_{ct}) of anode.

5.9. Confirmation of immobilisation of α-amylase and lysozyme using Cyclic Voltammetry

As shown in figure 5.12 the decrease in current values of cyclic voltammogram indicated the enzyme immobilization. Enzymes like α-amylase, lysozyme were immobilized on the PANI/rGO/Graphite paste/Al electrode surface. The decrease in CV current values indicated that the enzymes were immobilized over the electrode surface resulting an increase in the overall resistance value of the electrode.

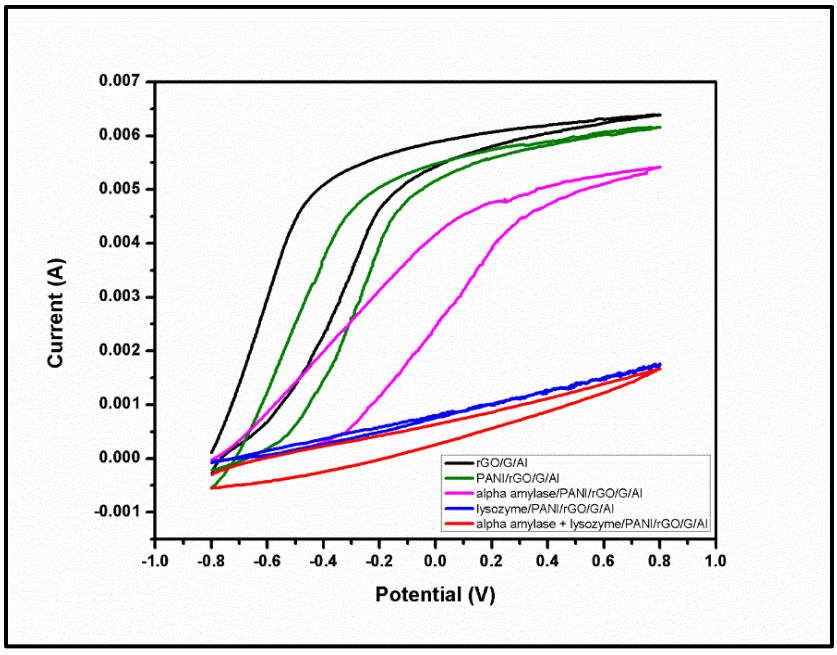

Figure 5.12 Immobilisation of alpha amylase and lysozyme over PANI/rGO/Graphite paste/Al electrode

5.10. Potential across 10 kΩ resistance vs time plots for miniaturized MFCs using different anode materials.

Potential vs time plots were made for MFCs using different anode materials like Graphite paste/Al, Graphite powder/Al, Graphite paste + powder/Al, PANI/rGO/Graphite powder/Al, rGO/Graphite paste/Al, PANI/rGO/Graphite paste/Al, α amylase + lysozyme/PANI/rGO/Graphite powder/Al with and without artificial saliva added and PANI/rGO/Graphite paste/Al with and without natural saliva added.

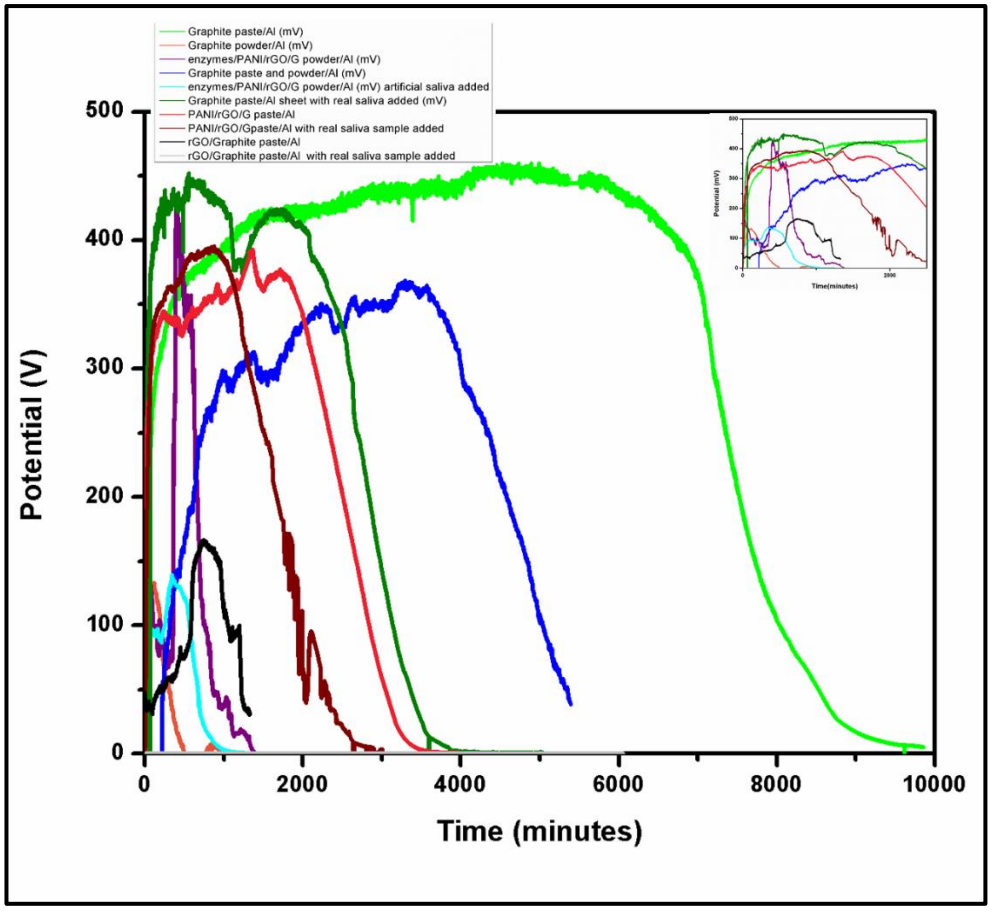

Figure 5.13 Potential (mV) vs time (minutes) plot for miniaturized MFCs using different anode materials

rGO/Graphite paste/Al exhibit high voltage with time as compare to graphite paste/Al. Thus, supporting previous results of electrode conductivity measurement indicating that rGO substrate is compatible to the potato fermenting microbes. Decrease in potential value attained in PANI further indicate low microbial growth over this substrate, PANI depecting antimicrobial activities. These results further matches to that of SEM results.

Instantaneous enhancement of Potential values were attained after adding saliva. Similar results were obtained when study was conducted with the electrodes having immobilized enzymes of lysozyme and alpha-amylase.

Thus enhancement of Potential is mainly due to presence of salivary enzymes as no substantial increase in current was observed when only artifial saliva was used.

5.11. Current through 10 kΩ resistance vs time plots for miniaturized MFCs using different anode materials.

Peak current of around 53.4 µA was measured in case of rGO/Graphite paste/Al. When the current value lowered real saliva was added to the anode resulting to an increase in the current value of the cell. Similarly, other electrode materials like Graphite powder/Al, rGO/Graphite paste/Al and PANI/rGO/Graphite paste/Al were also tested with and without saliva and they also showed an increase in the current value of the cell.

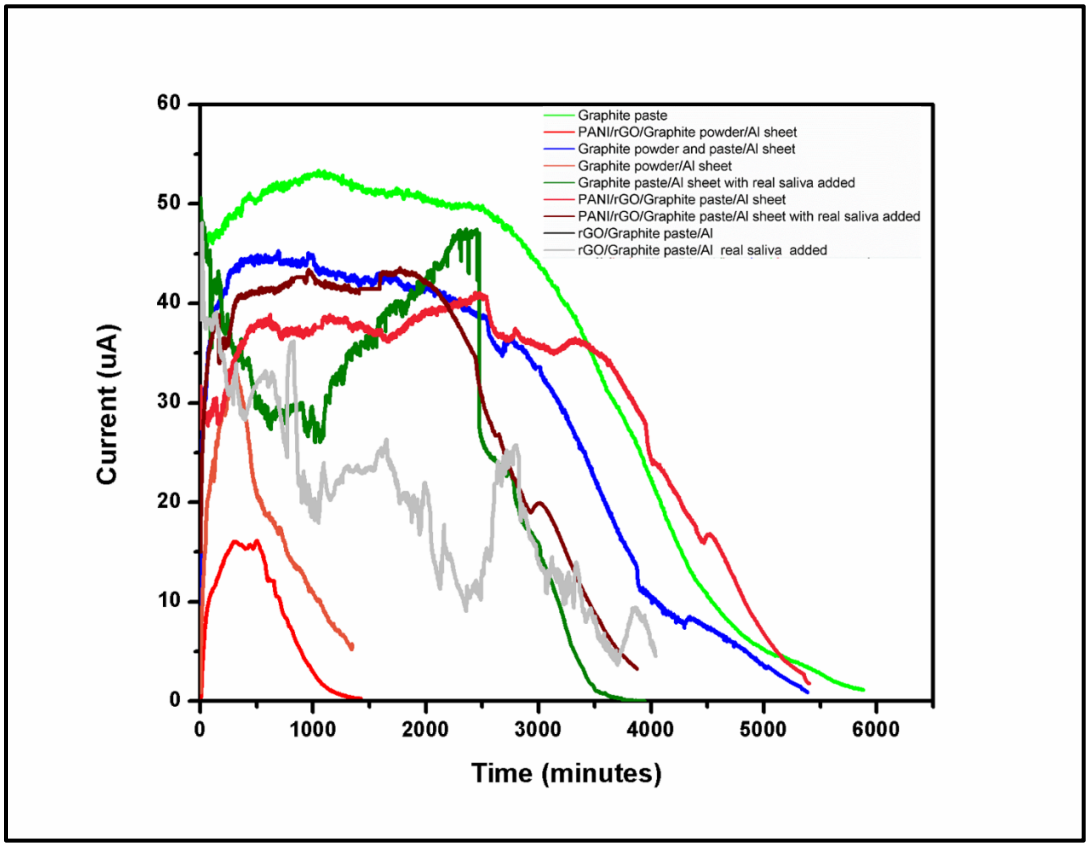

Figure 5.14 Current (μA) vs time (minutes) plot for miniaturized MFC for current passing through 10 kiloohm resistance

5.12. Reusability study of miniaturized MFC developed

Reusability study for miniaturized MFC was done by running the miniaturized MFC for 2 cycles i.e. fresh anolyte was added on the anode, once the MFC shows 0 potential after the first run. Measurements were made in terms of Potential (V) vs time(minutes). The potential in the second cycle also increased by about 11.98% it shows that our MFC is not only reusable but improves its electricity generating capacity on multiple uses.

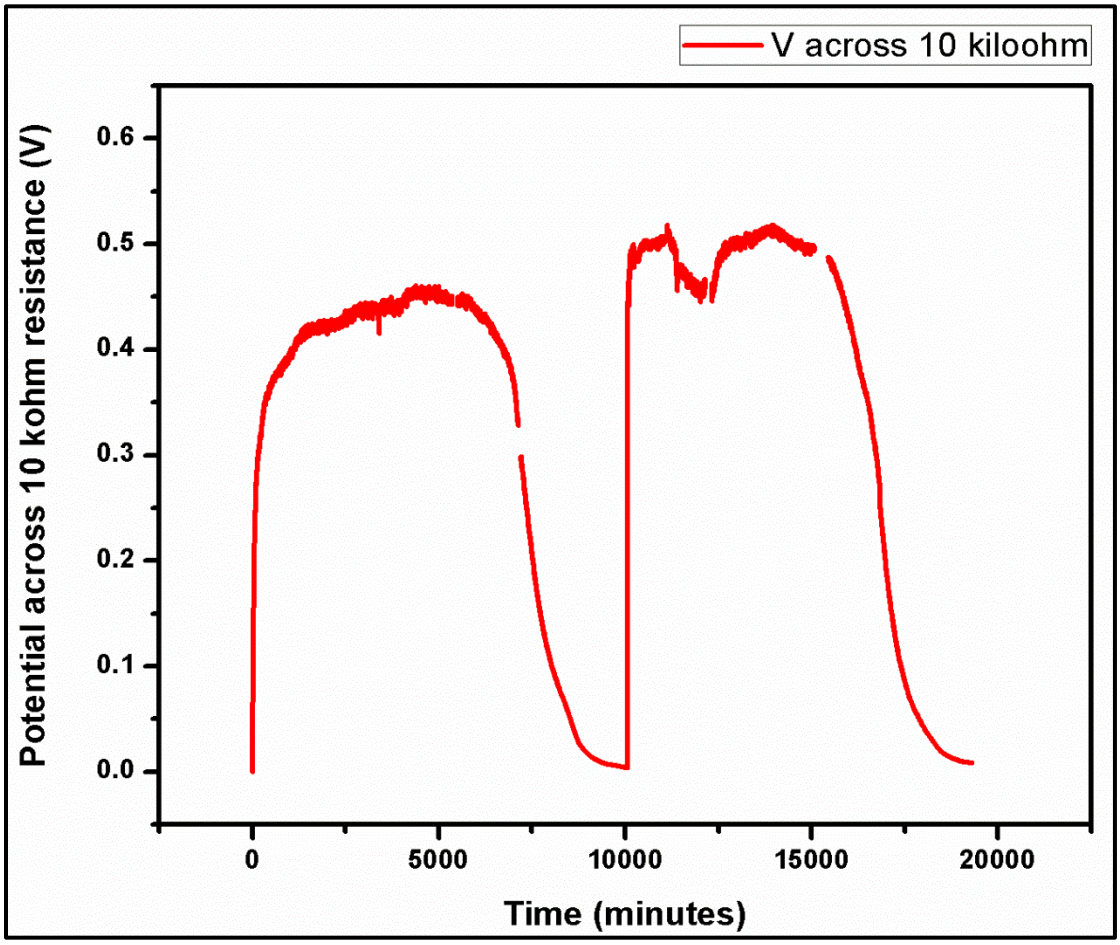

Figure 5.15 Potential (V) vs time (minutes) plot for Graphite paste/Al anode based miniaturized MFC for 2 cycles

5.13. Estimation of microbial growth in different electrode materials using spectrophotometry

Absorbance was measured at a wavelength of 546 nm using Perkin Elmer Lambda 950 UV-Vis-NIR spectrophotometer. Absorbance values at a dilution factor of 20 for microbes grown in different electrodes were found to be 0.962 for rGO/G/Al, 0.586 for alpha-amylase/rGO/G/Al, 0.594 for lysozyme/rGO/G/Al and 0.628 for alpha amylase+lysozyme/rGO/G/Al electrodes. Hence, microbial growth in rGO/G/Al electrode was maximum. Same electrode coated with enzymes like alpha amylase and lysozyme showed lower growth of microbes. Possible reason being the degradation of microbial membrane by the enzymes.

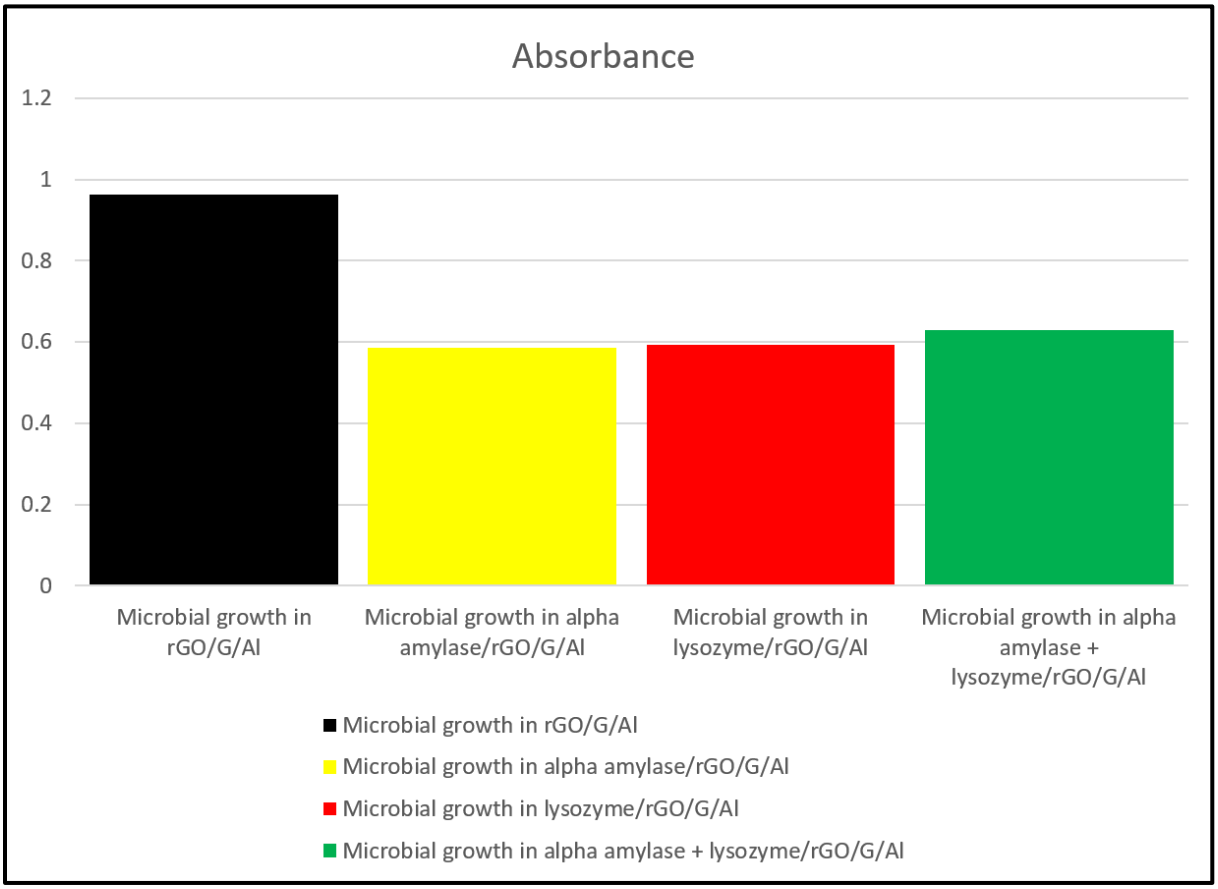

Figure 5.16 Absorbance vs time plot for microbial growth in different electrode materials

Table 5.6 Absorbance data of microbial culture grown over different electrode materials

Sr. No.	**Material over which mixed culture was grown**	**Absorbance**
1	rGO/Graphite paste/Al	.962
2	α amylase/rGO/Graphite paste/Al	.586
3	Lysozyme/rGO/Graphite paste/Al	.594
4	α amylase + lysozyme/rGO/Graphite paste/Al	.628

5.14. Energy Losses

Our device giving an OCV of 671.2 mV, peak current of 53 μA and an internal resistance of 1042.35 Ω was good enough to give an energy loss of 8% which is fairly good in case of membrane based MFC.

$$\boldsymbol{V_{device} = OCV - IR_{internal}} \qquad [\mathbf{32}]$$

$$\boldsymbol{V_{device} = 0.6712 - [(.000053)(1042.35)]}$$

$$\boldsymbol{V_{device} = 615\ mV}$$

$$\boldsymbol{Energy\ loss = 55.2\ mV}$$

Therefore,

$$\boldsymbol{Percentage\ Energy\ loss = \frac{Energy\ loss}{OCV} * 100}$$

$$\boldsymbol{Percentage\ Energy\ loss = \frac{55.2}{671.2} * 100}$$

$$\boldsymbol{Percentage\ Energy\ loss = 8.22\ \%}$$

The reason for energy loss being anode resistance, cathode resistance, membrane resistance and the resistance due to the electrolyte. The main reason for such a low energy loss being the extremely thin agar gel treated whatman filter paper based proton exchange membrane. Calculation of the energy losses in the graphite paste coated Al based system, we could better understand the maximum potential energy output under these conditions, as well as the possible

causes of energy loss in the system. The components of energy loss include the calculated resistances for the cathode, membrane, anode and electrolytes.

5.15. Shelf-life of miniaturized MFC

Shelf life study of miniaturized MFC was done and it was found that the MFC could run continuously for about 40 days. Hence, the shelf life of miniaturized MFC was 40 days. After this time period the Aluminium sheet used in the MFC degrades by the action of corrosion.

CHAPTER-6

6. CONCLUSIONS

From all of our above studies on Microbial Fuel Cells, we reached to the following conclusions:

- The MFC potential and current depends on the external load resistance to which the MFC is connected.
- The internal resistance (R_{in}) of an MFC decreases with time.
- The miniaturized MFC designed above is reusable has a shelf life of 40 days if used continuously.
- Human saliva containing enzymes like α-amylase and lysozyme acts on the microbes by degrading their cell membrane by lysozyme resulting in an immediate release of electrons from the cell membrane shuttle. Hence, resulting in a rapid increase in current and potential values.
- The energy loss associated with our device was 8.22%.

CHAPTER-7

6. FUTURE PERSPECTIVES

The principle of the BioCapacitor makes the possibility of practical applications for biofuel or enzyme fuel cells more realistic. Even though the biofuel cell is ecological and sustainable, a single cell will not theoretically generate sufficient electricity to operate currently available electronic devices, especially in the medical and healthcare fields. However, biofuel cells combined with a charge pump circuit and capacitor enable them to operate LEDs, radiotransmitters, and pumps, which are expected to be utilized in implantable devices in the medical field. Current cutting-edge studies of biofuel cells achieved further miniaturized electrodes with higher current densities together with advanced nanotechnology employment, utilizing glucose as well as acetaldehyde and cholesterol as the fuel to realize self-powered bio-sensing systems *in vitro* and *in vivo*. [30]

CHAPTER-8

7. REFERENCES

[1] *Z. Du, H. Li, and T. Gu, "A state of the art review on microbial fuel cells: A promising technology for wastewater treatment and bioenergy," Biotechnol. Adv., vol. 25, no. 5, pp. 464–482, Sep. 2007.*

[2] *M. Á. Fernández de Dios, A. G. del Campo, F. J. Fernández, M. Rodrigo, M. Pazos, and M. Á. Sanromán, "Bacterial–fungal interactions enhance power generation in microbial fuel cells and drive dye decolourisation by an ex situ and in situ electro-Fenton process," Bioresour. Technol., vol. 148, pp. 39–46, Nov. 2013.*

[3] *K. Rabaey and W. Verstraete, "Microbial fuel cells: novel biotechnology for energy generation," Trends Biotechnol., vol. 23, no. 6, pp. 291–298, Jun. 2005.*

[4] *B. Cercado-Quezada, M.-L. Delia, and A. Bergel, "Testing various food-industry wastes for electricity production in microbial fuel cell," Bioresour. Technol., vol. 101, no. 8, pp. 2748–2754, Apr. 2010.*

[5] *B. E. Logan, Microbial Fuel Cells. John Wiley & Sons, 2008.*

[6] *H. J. Mansoorian, A. H. Mahvi, A. J. Jafari, M. M. Amin, A. Rajabizadeh, and N. Khanjani, "Bioelectricity generation using two chamber microbial fuel cell treating wastewater from food processing," Enzyme Microb. Technol., vol. 52, no. 6–7, pp. 352–357, May 2013.*

[7] *L. Alzate-Gaviria, "Microbial Fuel Cells for Wastewater Treatment," Diss Yucatan Cent. Sci. Res. Nd Np Microb. Fuel Cells Waste Water Treat. Web.*

[8] *J. Wei, P. Liang, and X. Huang, "Recent progress in electrodes for microbial fuel cells," Bioresour. Technol., vol. 102, no. 20, pp. 9335–9344, Oct. 2011.*

[9] *L. Liu, O. Tsyganova, D.-J. Lee, J.-S. Chang, A. Wang, and N. Ren, "Double-chamber microbial fuel cells started up under room and low temperatures," Int. J. Hydrog. Energy, vol. 38, no. 35, pp. 15574–15579, Nov. 2013.*

[10] *L. Zhuang, S. Zhou, Y. Wang, C. Liu, and S. Geng, "Membrane-less cloth cathode assembly (CCA) for scalable microbial fuel cells," Biosens. Bioelectron., vol. 24, no. 12, pp. 3652–3656, 2009.*

[11] *T. T. Ngo, T. L. Yu, and H.-L. Lin, "Nafion-based membrane electrode assemblies prepared from catalyst inks containing alcohol/water solvent mixtures," J. Power Sources, vol. 238, pp. 1–10, Sep. 2013.*

[12] *J.-H. Won, H.-J. Lee, J.-M. Lim, J.-H. Kim, Y. T. Hong, and S.-Y. Lee, "Anomalous behavior of proton transport and dimensional stability of sulfonated poly(arylene ether sulfone) nonwoven/silicate composite proton exchange membrane with dual phase co-continuous morphology," J. Membr. Sci., vol. 450, pp. 235–241, Jan. 2014.*

[13] *Logan, Bruce E. "Exoelectrogenic bacteria that power microbial fuel cells." Nature Reviews Microbiology 7, no. 5 (2009): 375-381.*

[14] *A. González del Campo, P. Cañizares, M. A. Rodrigo, F. J. Fernández, and J. Lobato, "Microbial fuel cell with an algae-assisted cathode: A preliminary assessment," J. Power Sources, vol. 242, pp. 638–645, Nov. 2013.*

[15] *K. Scott, C. Murano, and G. Rimbu, "A tubular microbial fuel cell," J. Appl. Electrochem., vol. 37, no. 9, pp. 1063–1068, 2007.*

[16] *D. Zhang, F. Yang, T. Shimotori, K.-C. Wang, and Y. Huang, "Performance evaluation of power management systems in microbial fuel cell-based energy harvesting applications for driving small electronic devices," J. Power Sources, vol. 217, pp. 65–71, Nov. 2012.*

[17] *Y. Ahn and B. E. Logan, "Domestic wastewater treatment using multi-electrode continuous flow MFCs with a separator electrode assembly design," Appl. Microbiol. Biotechnol., vol. 97, no. 1, pp. 409–416, 2013.*

[18] *M. A. Rodrigo, P. Cañizares, J. Lobato, R. Paz, C. Sáez, and J. J. Linares, "Production of electricity from the treatment of urban waste water using a microbial fuel cell," J. Power Sources, vol. 169, no. 1, pp. 198– 204, Jun. 2007.*

[19] *Sode, K., Yamazaki, T., Lee, I., Hanashi, T., & Tsugawa, W. (2016). BioCapacitor: A novel principle for biosensors. Biosensors and Bioelectronics, 76, 20-28.*

[20] *Fraiwan, Arwa, Sayantika Mukherjee, Steven Sundermier, Hyung-Sool Lee, and Seokheun Choi. "A paper-based microbial fuel cell: Instant battery for disposable diagnostic devices." Biosensors and bioelectronics 49 (2013): 410-414.*

[21] *Rabaey, K.; Boon, N.; Siciliano, S. D.; Verhaege, M.; Verstraete, W. Biofuel cells select for microbial consortia that self-mediate electron transfer. Appl. Environ. Microbiol. 2004, 70, 5373-5382.*

[22] *Park, H. S.; Kim, B. H.; Kim, H. S.; Kim, H. J.; Kim, G. T.; Kim, M.; Chang, I. S.; Park, Y. K.; Chang, H. I.A novel electrochemically active and Fe(III)-reducing bacterium*

phylogenetically related to Clostridium butyricum isolated from a microbial fuel cell. Anaerobe 2001, 7, 297-306.

[23] Fricke, Katja, Falk Harnisch, and Uwe Schröder. "On the use of cyclic voltammetry for the study of anodic electron transfer in microbial fuel cells." Energy & Environmental Science 1, no. 1 (2008): 144-147.

[24] "Technology and Application of Microbial Fuel Cells." (2014).

[25] Logan, Bruce E., Bert Hamelers, René Rozendal, Uwe Schröder, Jürg Keller, Stefano Freguia, Peter Aelterman, Willy Verstraete, and Korneel Rabaey. "Microbial fuel cells: methodology and technology." Environmental science & technology 40, no. 17 (2006): 5181-5192.

[26] Reguera, G.; McCarthy, K. D.; Mehta, T.; Nicoll, J. S.; Tuominen, M. T.; Lovley, D. R. Extracellular electron transfer via microbial nanowires. Nature 2005, 435, 1098-1101.

[27] Sekar, Narendran, and Ramaraja P. Ramasamy. "Electrochemical impedance spectroscopy for microbial fuel cell characterization." J Microb Biochem Technol S 6, no. 2 (2013).

[28] Fan, Yanzhen, Evan Sharbrough, and Hong Liu. "Quantification of the internal resistance distribution of microbial fuel cells." Environmental science & technology 42, no. 21 (2008): 8101-8107.

[29] *Manohar, Aswin K., Orianna Bretschger, Kenneth H. Nealson, and Florian Mansfeld. "The use of electrochemical impedance spectroscopy (EIS) in the evaluation of the electrochemical properties of a microbial fuel cell." Bioelectrochemistry 72, no. 2 (2008): 149-154.*

[30] *Brownson, Dale AC, and Craig E. Banks. The handbook of graphene electrochemistry. London: Springer, 2014.*

[31] *Del Campo, A. González, P. Cañizares, J. Lobato, M. Rodrigo, and FJ Fernandez Morales. "Effects of External Resistance on Microbial Fuel Cell's Performance." In Environment, Energy and Climate Change II, pp. 175-197. Springer International Publishing, 2014.*

[32] *Mink, Justine E., Ramy M. Qaisi, Bruce E. Logan, and Muhammad M. Hussain. "Energy harvesting from organic liquids in micro-sized microbial fuel cells." NPG Asia Materials 6, no. 3 (2014): e89.*

[33] *Wei, Jincheng, Peng Liang, and Xia Huang. "Recent progress in electrodes for microbial fuel cells." Bioresource technology 102, no. 20 (2011): 9335-9344.*

[34] *F. Zhang, S. Cheng, D. Pant, G. V. Bogaert, and B. E. Logan, "Power generation using an activated carbon and metal mesh cathode in a microbial fuel cell," Electrochem. Commun., vol. 11, no. 11, pp. 2177–2179, 2009.*

[35] *A. Dewan, H. Beyenal, and Z. Lewandowski, "Scaling up microbial fuel cells," Environ. Sci. Technol., vol. 42, no. 20, pp. 7643–7648, 2008.*